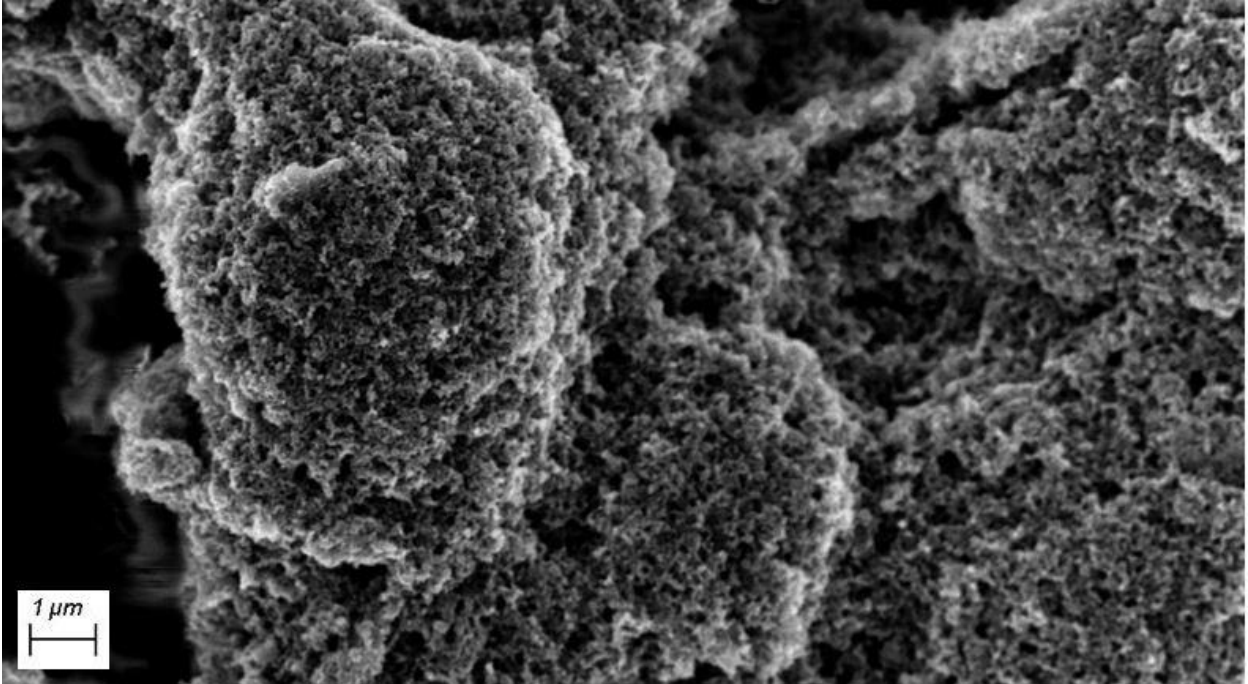




CHALMERS
UNIVERSITY OF TECHNOLOGY



Exploring factors for electrode prototyping for PEM fuel cells

Master's thesis in Material Chemistry

Frederikke Björklund Larsen

DEPARTMENT OF PHYSICS

CHALMERS UNIVERSITY OF TECHNOLOGY
Gothenburg, Sweden 2024
www.chalmers.se

MASTER'S THESIS 2024

Exploring factors for electrode prototyping for PEM fuel cells

FREDERIKKE BJÖRKLUND LARSEN



CHALMERS
UNIVERSITY OF TECHNOLOGY
Department of Physics
Division of Chemical Physics
Chalmers University of Technology
Gothenburg, Sweden 2024

Exploring factors for electrode prototyping for PEM fuel cells
FREDERIKKE BJÖRKLUND LARSEN

© FREDERIKKE BJÖRKLUND LARSEN, 2024.

Supervisor: Parinaz Mikaeili, PowerCell Group AB
Examiner: Björn Wickman, Department of Physics

Master's Thesis 2023
Department of Physics
Division of Chemical Physics
Chalmers University of Technology
SE-412 96 Gothenburg
Telephone +46 31 772 1000

Cover: SEM image of 50 μm coatings of Ink1 after one day of maturation on glass fibre reinforced decal, taken with x15 000 magnification and has a scale bar of 1 μm . Image was taken with the help of Nils Rieger.

Exploring factors for electrode prototyping for PEM fuel cells
FREDERIKKE BJÖRKLUND LARSEN
Department of Physics
Chalmers University of Technology

Abstract

As the world push to lower carbon dioxide emissions to limit climate change, the need for new technologies becomes more and more critical. Some emerging technology is hydrogen fuel cells and amongst them are proton exchange membrane fuel cells. With all new technologies there are several factors that need development, and this work takes a closer look at the catalyst layer of the cathode. Setting out to increase the platinum loading in the cathode while at the same time avoiding cracks, several catalyst inks were made with varying dispersion matrices. The matrices explored were a) water with ethanol and 1-propanol (2:2:1 weight ratio), b) water with 1-propanol (2:3 weight ratio), c) water with 2-propanol (2:3 weight ratio), d) water with tert-butanol (2:3 weight ratio), e) water with 1-propanol and tert-butanol (2:1:2 weight ratio), and f) water with 1-propanol and tert-butanol (1:1:3 weight ratio).

To get a deeper understanding of the ink's properties, rheological tests of the inks and visual analysis of produced electrodes were performed. These analyses found improved coating quality and a higher viscosity for dispersions with a lower dielectric constant and for inks containing solvent with a lower vapour pressure. The improved behaviour was attributed to improved interactions between the ink's compounds and slower drying of the coatings, leading to less stresses in the electrodes. An improved electrode quality was also observed when the inks were left to mature on a magnetic stirrer for several days. The maturation step resulted in lower viscosity of the inks indicating smaller effective volume fraction of particles and less electrostatic repulsion and steric hinderance between compounds. A final factor in the process that was tested was increasing the relative humidity during the drying process. Here an improved cracking behaviour was observed for the ink containing more water while the opposite was seen in the ink containing more tert-butanol. These findings point towards the need for specific drying processes for each individual ink.

Acknowledgements

First, I would like to give a big thank you to my two supervisors Parinaz Mikaeili and Felix Ernst for their guidance and support, both on the factual and the emotional sides, as well as my examiner Björn Wickman. To Nils Rieger and Marcus Liljenberg, thank you for your support and guidance during the SEM session. I would also like to say thank you to the rest of the MEA development team at PowerCell Group AB for all the interesting discussions, they have been of great help. I'd like to give a special thanks to the interns and other thesis students at PowerCell Group AB, thank you for all the laughs and the good times. Thank you to everyone at PowerCell Group AB for the warm welcome.

Lastly, I would like to say a big thank you to my friends and family. Thank you for the support and keeping me focused, and the distraction when needed.

Frederikke Björklund Larsen, Gothenburg, December 2023

Abbreviations

CL	Catalyst layer
FOV	Field of view
HSAC	High surface area carbon
IPA	2-Propanol
LVER	Linear viscoelastic region
NPA	1-Propanol
PEMFC	Polymer electrolyte membrane fuel cell
PFSA	Perfluorosulfonated acid
PTFE	Polytetrafluoroethylene
RH	Relative humidity
RS	Roller shaker
TB	tert-Butanol
US	Ultrasonicator
wt.%	Weight percentage

Table of Contents

Abstract.....	IV
Acknowledgements.....	VII
Abbreviations.....	IX
1 Introduction.....	1
1.1 Aim.....	1
1.2 Demarcation.....	1
2 Theory.....	3
2.1 Working principle of a fuel cell.....	3
2.2 Electrode compounds.....	4
2.2 Dispersion.....	5
2.2.1 Ultrasonication.....	5
2.2.2 Roller shaker.....	5
2.3 Processing steps.....	6
2.3.1 Maturation.....	6
2.3.2 Coating.....	6
2.5 Physical characterisation/Microscope.....	9
3 Method.....	10
3.1 Material.....	10
3.2 Ink preparation.....	10
3.3 Dispersion.....	10
3.4 Rheological test.....	11
3.5 Film application and drying.....	11
3.6 Light microscopy.....	12
3.7 Scanning electron microscope.....	12
4 Results and discussions.....	13
4.1 Dispersion matrix.....	13
4.1.1 HEN:221 inks.....	13
4.1.2 Impact of alcohol on coating quality.....	15
4.1.3 HNT:212 inks.....	18
4.1.4 HNT:113 inks.....	22
4.2 Processing of the inks.....	26
Conclusion.....	28
Outlook.....	28
References.....	30
Appendix.....	I

1 Introduction

With the world moving away from fossil fuels we need to find alternative ways of securing the transport for people and goods. Batteries may be the technology that first comes to mind, and while batteries are suitable for lighter applications and shorter distance, innovative technology is needed when it comes to heavier transports and stationary applications [1]. An alternative is hydrogen fuel cells which is becoming an increasingly more reliable option. The technology takes advantage of the energy released when hydrogen is combined with oxygen to form water and converts this energy into electricity.

This work was conducted at PowerCell Group AB, from hereon called PowerCell, where they focus on developing hydrogen fuel cells for a variety of applications including aviation and marine [2]. The first hydrogen-oxygen fuel cells were created during the 1830's, though the use of the cells have been limited and development has therefore been slow [3]. Some of the limiting factors for further development and use, is the lack of infrastructure to distribute hydrogen, and the production of hydrogen from renewable sources. One policy that will help at least with hydrogen production is that the EU aims to have 20 million tonnes of its hydrogen consumption made from renewable resources by 2030 [4]. Other factors limiting the use of hydrogen fuel cell are the high price of the fuel cell compared to its performance and poor durability [3]. Another factor is ensuring a high enough energy output while at the same time having a high utilisation of the catalyst used to enable the reaction. The catalyst currently used is typically platinum which not only is expensive, is also used in many other applications and is a limited resource [5].

A fuel cell works by converting chemical energy into electrical energy through a catalytic process [1]. It has some advantages over other forms of energy conversion like not being limited by the Carnot conversion, such as a combustion engine is. While there are several types of fuel cells, this work will focus on the hydrogen fuel cell where hydrogen reacts with oxygen to form only water, electrical current and heat as its products. The type of hydrogen fuel cell that will be investigated here is the so-called proton exchange membrane fuel cell (PEMFC), with the thesis more specifically focusing on the catalytic inks used for electrode production. The electrodes are a small but significant part of the PEMFC.

1.1 Aim

The aim of this thesis is to continue the work of understanding the interactions between components in catalytic inks form PEMFC electrodes. The thesis investigates how combining methods of dispersion of the components and how adjusting dispersion matrix composition can help achieve the optimal electrode properties. It continues the work done by Nora Malmquist [6], Emma Ulberstad [7] and Sandeep Jayaprakash Nair [8] for each of their thesis. More specifically, this thesis focuses on exploring variables in the process and the dispersion matrix used, and their impact on the electrode coatings properties. This thesis investigates different alcohols used in the dispersion matrix as well as the ratio of the solvents used. Regarding the processing variables, the thesis investigates different maturation times. The properties that are explored include the rheological behaviour of the inks and the quality of the resulting electrodes.

1.2 Demarcation

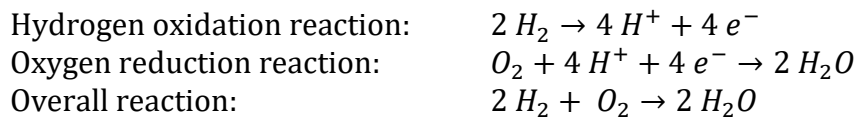
This thesis does not focus the broader challenges of the hydrogen industry, for example issues related to production and distribution of hydrogen. Neither does it explore other parts of the PEMFC outside of the catalyst coating on the electrodes. It is limited to one commercially

available catalyst and one binder. The work focuses on the behaviour of the mixed inks and not how individual component interact. The tests were also only performed once, and the reproducibility has not been explored. The analysis methods used only give part of the explanation and are not accurate enough to give the full explanation to the cause of observed behaviours. Instead, this work attempts to give suggestions to the cause of the trends observed in the results.

2 Theory

2.1 Working principle of a fuel cell

The PEMFC is built up of an anode, a membrane and a cathode formed into a catalyst coated membrane [1]. The working principle behind PEMFC is shown in Figure 2.1. Molecular hydrogen is split by a catalyst into protons and electrons on the anodic electrode, and the protons travel through the membrane. The electrons are transported over to the other side of the membrane by passing around it, through an electric circuit. Once on the other side of the membrane, the electrons are combined with the protons and oxygen on the cathodic electrode to form water, again with the help of a catalyst. The reactions in the cell are as stated:



The first reaction is the anodic half-reaction, the second reaction is the cathodic half-reaction, and the third reaction is the overall reaction [1]. It is the flow of the electrons that generates the current which can then be utilised in for example a motor. The cathodic half-reaction requires both the breaking of the double bond in molecular oxygen and four electrons to happen which result in voltage losses. To minimise these losses the cathode generally requires more help in the form of a higher catalyst loading. Increasing the catalyst loading can be difficult, so this study will focus on achieving a higher catalyst loading for the cathodic side of the PEMFC.

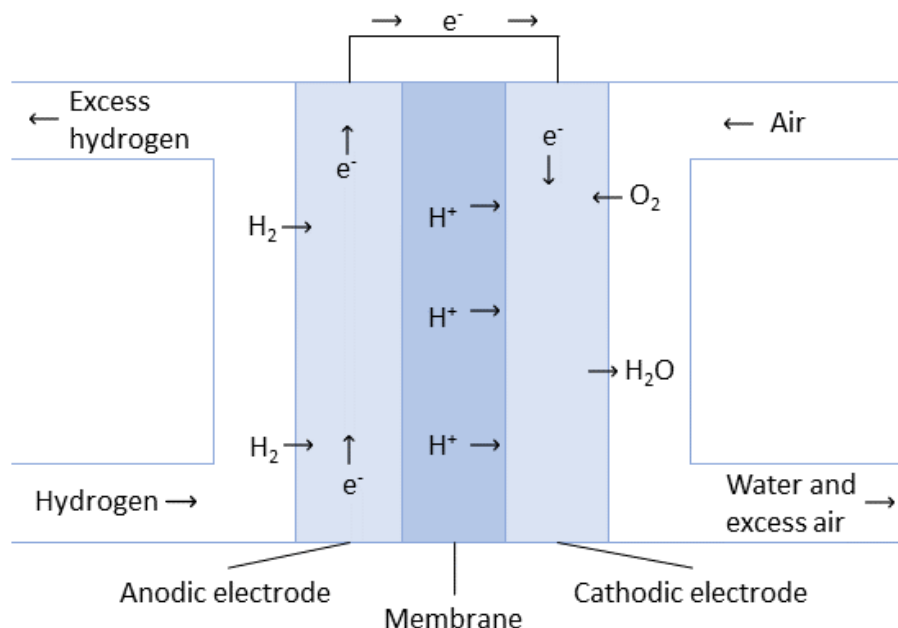


Figure 2.1. Schematic figure of PEMFC and the flow of reactants and products.

The electrodes are built up of a dispersion of a solvent matrix, a catalyst, and binder, which here is an ionomer, and this dispersion is often referred to as an ink [9]. The ink is then coated on a decal to form electrodes. The catalyst used in PEMFC is platinum particles dispersed on a carbon substrate. The ionomer often used is a copolymer with a backbone of polytetrafluoroethylene (PTFE) and side chains of perfluorosulfonated acids (PFSA). A key feature of the ionomer is that the sidechains have a sulphonic group that lose a proton when in

an aqueous environment. This negative charge allows the proton to move between sulphonic groups, to and from the catalyst, and thereby move through the electrodes. To increase the efficiency of the fuel cell the cathodic electrode needs a homogeneous coating with a high catalyst loading [9]. A higher catalyst loading can be achieved either by increasing the amount of catalyst in the ink, the so-called solid content, or by having thicker coatings. Increasing the solid content tends to result in poor electrodes with ineffective catalyst usage and poor durability. This study will focus on how to achieve thicker coatings while maintaining a homogenous coating on the electrodes with minimal cracks.

2.2 Electrode compounds

The choice of the compounds has a major impact on the resulting electrodes. The compounds can seem very similar at first glance when in truth the interactions between them vary wildly. For example, several studies have explored how the ionomer in Nafion D2020 solution forms in different solvents [9, 10, 11, 12]. A main property these studies discuss is how the dielectric constant (ϵ) influences the inks. The dielectric constant is closely related to the polarity of the solvents and impacts the interactions between the dispersion matrix and the ionomer, and the catalyst. The theory is that the ionomers tend to curl up into tight coils in solvents with high dielectric constant due to poor interactions between the solvent and the fluorinated carbon chains that make up the backbone and large parts of the sidechains. So, comparing water, with a dielectric constant of 78.4, to tert-butanol (TB), with a dielectric constant of 10.9, the latter would cause the ionomer to stretch out more. The looser structure should result in a more ionomer-ionomer-interactions and more entanglements, resulting in a larger viscosity. On the other hand, if the dielectric constant is too small ($\epsilon < 3$) the ionomer will form a precipitate due to the polar sulphonic groups on the sidechains. The impact of the dielectric constant on the ionomer highlights the need for a suitable dispersion matrix. For simplicity the dielectric constant of a matrix will be calculated through a weighted average of the compounds in the matrix [13].

Another factor that is discussed in studies is how the drying process impacts crack formation [9]. Previous work at PowerCell found that increasing the partial pressure of the alcohol used in the dispersion matrix during the drying process, can minimise crack formation [8]. It works by lowering the driving force for the alcohol to evaporate which slows down the drying process. The longer drying time causes less cracks to form from internal stresses, i.e., stress cracks. It could therefore be argued that having a solvent matrix containing compounds with lower vapour pressure would have a similar impact as the ink would dry slower. As having a lot of organic solvent vapour would be impractical in a larger production, increasing the relative humidity (RH) during drying could be a method for controlling crack formation. Presented in Table 2.1 are the dielectric constant and vapour pressure of the solvents used. 1-propanol (NPA), 2-propanol (IPA), ethanol and TB has previously been used at PowerCell and are therefore also used here [6, 7]. Other properties such as the structure of the solvent should also be taken into consideration, for example the symmetrical structure of IPA compared to the asymmetrical structure of NPA [14].

Table 2.1. Dielectric constant and vapour pressure of water, NPA, IPA, ethanol, and TB

Property	Water	NPA	IPA	Ethanol	TB
Dielectric constant, ϵ	78.4	20.1	20.1	25.3	10.9
Vapour pressure, as 25 °C (hPa)	18	19	43	59	36

2.2 Dispersion

To ensure a homogeneous dispersion of the components in the ink, the dispersion method becomes especially important [15]. The carbon support of the catalyst particles is hydrophobic, so the catalyst tends to form aggregates in polar solvents to avoid interactions with the dispersion matrix. In these catalyst structures there are the micropores in the carbon support, mesopores between the individual catalyst particles, and macropores that form in larger aggregates which are on the micron-scale [16]. These aggregates need to be broken down to get a good utilisation of the catalyst and can be done with an ultrasonicator (US) and/or roller shaker (RS). These aggregates also tend to cause cracks which result in poor durability.

2.2.1 Ultrasonication

The US works by oscillating a metal rod, called a sonotrode, at a specific frequency but with varying amplitude in the sample, where increased amplitude or time of US increases the energy input [17]. The oscillation causes alternating compression and refraction cycles that generate bubbles with negative pressure when the sonotrode moves up. With enough oscillation the bubbles aggregate and cause a cavitation bubble. The cavitation bubbles become unstable and implode, resulting in jets of the liquid. These jets have enough energy to overcome the intermolecular forces and cause larger aggregates to break. The US measures the energy required to oscillate the sonotrode through the medium, and the energy input depends on the thickness of the ink mixed, the amplitude at which the sonotrode oscillates and the size of the sonotrode. The US is chosen over an ultrasonic bath as it generates higher energies and is more aggressive resulting in more dispersed inks [15].

2.2.2 Roller shaker

The RS mixes the dispersion by adding ceramic beads to the sample vial and is placed on rotating rods. The RS rotates the vial around its axis while being rocked back and forth [15]. This movement causes the beads to roll around and mechanically grind down the aggregates as the beads collide. How well the aggregates are broken down are dependent on the speed and mass of the beads as it impacts the energy at which the beads collide. The viscosity of the ink is also important as a higher viscosity would slow down the beads, lowering their kinetic energy [18]. The roller shaker has a limit to how small it can grind down the aggregates due to the inter-bead space created when three beads are touching, see Figure 2.2. The inter-bead space increases with larger beads used.

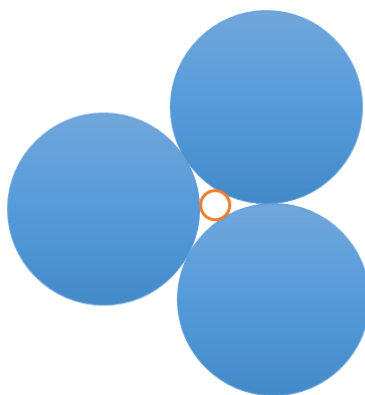


Figure 2.2. Inter-bead space marked in orange ring between beads in filled blue.

By understanding how the dispersion method can be optimised and how factors impact, the future fabrication of catalyst inks can be customised for specific applications. These factors

include energy input during US, the size (and thereby the weight) of the beads used during RS, the total weight of the beads in relation to the weight of the ink and processing time [19].

2.3 Processing steps

Aside from ensuring a proper mixing of the compounds, the impact of other processing steps can have major impacts on the resulting coatings quality. Some, that have been explored here, include maturation time, the coating process, and the drying process.

2.3.1 Maturation

While maturation has been poorly described in literature, previous results at PowerCell has shown great changes in the cracking behaviour of the coatings with increased maturation time. The process consists of, after the dispersing steps, leaving the sample vial with agitation for a set amount of time. In this work the sample was placed on a magnetic stirrer. Due to the ink's unstable dispersion nature, they cannot be left without agitation for too long as the compounds will separate causing a non-uniform ink. Exactly how different methods impact the electrode quality and how long a quality coating can be ensured has not been thoroughly studied. To analyse what exactly happens on a molecular level in the ink is difficult, in part due to the dark colour of the inks which are a result of the carbon support of the catalyst. Furthermore, I was not able to find any works explaining what happens during maturation so I will present some suggestions in this work. Some studies have though shown that during the mixing step the organic solvents oxidise in the presence of the catalyst creating several other compounds [20]. During a degassing step these new compounds were expelled from the ink which changes the interactions between the compounds. A potential reason for a change in electrode quality could be that with more maturation time, more solvent oxidises which changes the composition in the ink and thereby its behaviour.

2.3.2 Coating

There are many methods used for coating a catalyst ink onto decals to form the electrodes, and the one used at PowerCell is the doctor blade with a film applicator. The coating step is important because it determines which properties the ink needs to have, such as viscosity and modulus [9]. When using the doctor blade to coat, the ink is exposed to a shear that depends on the gap height and the coating speed.

Another important factor is onto which decal the ink is coated. Both the materials properties, such as surface energy, and the structure of the reinforcement of the decal impacts [9]. For example, if the decal uses glass fibres in the reinforcement the fibres can cause patterns and cracks in the electrode coating that follow the woven glass fibres peaks and valleys. Such patterns can be seen in Figure 2.3 where the same ink has been coated at the same thickness on a decal with glass fibres support versus one with PET support that has no such patterns.

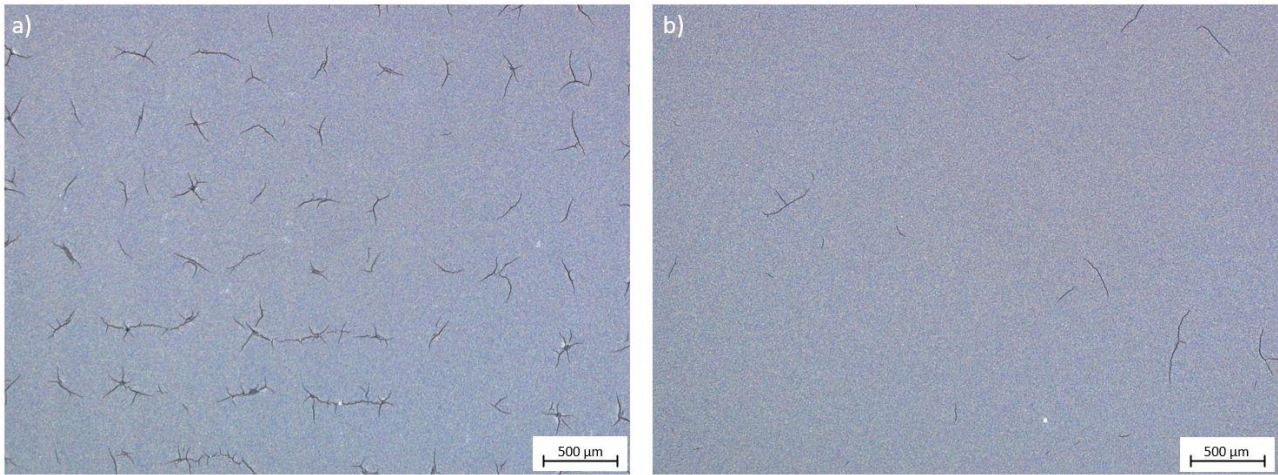


Figure 2.3. The same ink coated on a) decal with glass fibre reinforcement, and b) decal with PET backing.

2.3.3 Drying

A major impact on the electrode's quality and how cracks form, is under which conditions the electrode coatings are allowed to dry [8, 9]. The cracks are often divided into defect cracks and stress cracks. Defect cracks originate in defects such as aggregates, dust and impurities, and stress cracks that form from internal stresses caused by the drying process. It is mainly the stress cracks that can be controlled with the drying conditions. Cracks formed due to defects can be minimised by having a clean working environment and a well dispersed ink. Imperfections are hard to completely avoid but controlling the spread of any resulting cracks are important for ensuring the quality during electrode production.

2.4 Rheology

Rheology is the science of how semi-solids and liquids deform, and such measurement can help describe structures in the sample [21]. Both the sample's viscosity and viscoelastic properties can be used to help describe these structures. Viscosity and viscoelasticity can be measured using a rotating method where the liquid is sandwiched between a cone-and-plate set up; the cone on top rotates while the bottom plate remains stationary. The rotation of the cone results in a shear force (F) which gives a shear stress (σ) over a specific area, see Equation 1. The shear rate (γ) is given by dividing the velocity (v) by the distance between the plates (h) see Equation 2. In the rheometer the velocity is the rotational speed at each measuring point. The shear viscosity (η) is then giving by the shear stress over a given shear rate, see Equation 3. By varying the shear rate and measuring the response the liquids properties can be characterised.

$$\sigma = \frac{F}{A} \quad (1)$$

$$\gamma = \frac{v}{h} \quad (2)$$

$$\eta = \frac{\sigma}{\gamma} \quad (3)$$

Here the shear stress (σ) is in Pa, shear force (F) is in N, the specific area (A) is in m^2 , shear rate (γ) is in s^{-1} , velocity (v) is in m/s , height difference (h) is in m, and shear viscosity (η) is in $\text{Pa}\cdot\text{s}$.

The other key property, the viscoelastic behaviour of the liquid, is measured through an oscillating measurement [22]. In a fully viscous material, the deformation of the material would

be constant for an applied stress and the deformation remains after the stress is removed. The energy of the applied stress is therefore dissipated throughout the sample. On the other hand, a fully elastic material has no dissipation of energy when the load is applied, and it would therefore spring back to its shape with lowest energy after the strain is removed. For materials that fall in between these two categories a more complete picture is given of how a liquid responds to deformation by measuring the viscoelastic property. By oscillating the cone around the sample's equilibrium point at varying stress amplitude or frequency the applied strain to stress is measured. From there the complex modulus (G^*), in Pa·s, can be calculated with Equation 4 [21].

$$G^* = \frac{\sigma_{max}}{\gamma_{max}} \quad (4)$$

The storage modulus (G'), in Pa·s, a measure of the elastic property, can then be calculated according to the Equation 5 [21]. Similarly, the loss modulus (G''), in Pa·s, corresponds to the viscous component and can be calculated with Equation 6. In both equations δ is the phase angle which is the lag in the upper plate sinusoidal oscillation.

$$G' = G^* \cos(\delta) \quad (5)$$

$$G'' = G^* \sin(\delta) \quad (6)$$

If the response is perfectly in phase with the strain, $\delta=0$, resulting in $G'=G^*$ and $G''=0$, the response is purely elastic [22]. If $\delta=\pi/2$, resulting in $G'=0$ and $G''=G^*$, the response is completely out of phase resulting in a purely viscous response. If a sample has a higher storage modulus it is elastic-dominant and will be better at retaining its shape. This points to a stronger internal structure in the sample while the opposite can be said if the sample has a higher loss modulus, and therefore called viscous-dominant. The effect is that an elastic-dominant sample is harder to push through a nozzle, while a viscous-dominant sample might drip out of the nozzle instead. These properties tend to mirror each other, meaning that a high storage modulus tend to relate to a low loss modulus. Related to the viscous and elastic modulus are the linear viscoelastic region (LVER). In the LVER the viscoelastic properties are independent of the strain while above it the structure of the sample starts to break down due to the stress.

Though there is no direct correlation between the electrode quality and the rheological properties, rheological testing can give insight into the changes an ink goes through during processing. The inks can be seen as a colloidal dispersion of catalyst particles with ionomer to help the dispersion in a dispersion matrix. There could also be ionomers in self-assembled structures present that have no interaction with the catalyst. When it comes to colloidal dispersions, the electrostatic interactions have a large impact on the rheological behaviour [21]. Increasing the repulsing forces cause an increase in the effective radius of the particle which result in an increased zero-shear viscosity. The strength of the repulsion is dependent on the surface charge and the ionic strength of the particle, the of range of interactions and interactions between particles and the dispersion matrix. Decreasing the particle size cause the additional layer from the ionomer to have a larger impact of the rheology. As the shear increases the particles deform and the shear force becomes large enough to overcome the repulsing intermolecular forces and cause the ionomers to disentangle.

In a colloidal dispersion the rheological behaviour is also dependent on the size of the components, especially regarding steric hinderance [21]. The impact is dependent on the size of the molecules and the flexibility of it with larger and less flexible molecules increasing

viscosity. With large molecules such as the ionomer the size not only impacts the steric hinderance but also the diffusion rate of the molecule.

In a catalyst ink, having a higher viscosity could indicate a better solvent-ionomer interaction as improved interactions would cause the ionomer to stretch out and interact with other ionomers. The stretched-out ionomer could also increase interaction with the catalyst. The catalytic inks tend to display a shear thinning behaviour which is due the ionomers disentangle and align at higher shear causing them to slide past each other. The rheological behaviour is not directly translatable to the quality of coatings, but it can be used to compare inks and to ensure reproducible results.

2.5 Physical characterisation/Microscope

The electrodes are currently evaluated with a light microscope to assess their quality. Like the methods used by Lei et al. [14], the origin of the cracks formed can be characterised through a visual inspection. The light microscope has some limits though, mainly that the smallest objects possible to observe cannot be smaller than the wavelength of the light, the smallest size observable is about half a micron to a micron in size. It is currently not as much of an issue as at this point of the development, the aggregates and cracks formed tend to be bigger than one micron. Another limit is due to the carbon used as catalyst support cause the electrode to become jet black making it hard to see how the bulk of the catalyst layer (CL) is formed. Therefore, a scanning electron microscope (SEM) can be used to get more information and a closer look of the structure of the CL. The SEM uses electron with shorter wave lengths than visible light to map the sample in three ways [23].

1. Secondary electrons, they form when the incoming electron has an inelastic collision with the atom causing an inner electron to be ejected out from its orbit. These ejected electrons have a low energy allowing them to only travel a short distance. Therefore, they give insight into the surface of the sample.
2. Backscattered electrons, they originate from an elastic collision between the incoming electron and the atom. The incoming electron is flung around the nucleus and return from where it came, and then detected. The interaction volume is larger compared to the secondary electrons resulting in lower surface resolution. On the other hand, heavier atoms are better at generating these electrons resulting in a contrast between the elements present in the sample.
3. Characteristic x-rays, which are created as a secondary electron is ejected and one of the other electrons relaxes to fill the gap. The energy of these x-rays is characteristic for each element present and can therefore help determine the content of the sample and the distribution of the elements.

There are though some limits to these analysis methods. For example, having a large magnification allows for a detailed inspection but only on a very small area of the sample. Also, to get clear images with the SEM the sample needs to be conductive which includes having a proper connection between the sample and the sample holder. Additionally, there is currently no precise method for determining the number and size of cracks at PowerCell. It makes the characterisation arbitrary, dependent on the person performing the analysis and their experience.

3 Method

3.1 Material

The catalyst used had a platinum loading of 50 wt.% on a high surface area carbon (HSAC). The dispersion matrices explored were mixtures of deionised water, ethanol, 1-propanol (NPA), 2-propanol (IPA) and tert-butanol (TB). The ionomer used was an ionomer dispersion of a PTFE ionomer with long PFSA side chains. The weight of the ionomer dispersions content was subtracted from the weight of the dispersion matrix to get the wanted ratio. The inks were designed to have an ionomer/platinum ratio of 1, an ionomer/carbon ratio of 0.94 and a solid content of 12.6 wt.%. The inks were dispersed in plastic vials to ensure that the vials would not break while on the RS. Ink1-4 were coated on decals with a glass fibre reinforcement while Ink5 and Ink6 were coated on decals with PET support.

3.2 Ink preparation

The catalyst powder was first added to the plastic vial followed by the corresponding amount of deionised water was added. This order was used to avoid a flammable environment that a combination of organic solvent and the HSAC-based catalyst can create. The ionomer was then added and lastly the alcohol. A magnetic stir bar was added to ensure good mixing before and during the dispersing step. The inks total weight came to between 20 g and 35 g. The solvent matrices explored were 2:2:1 (w/w) H₂O/EtOH/NPA, 2:3 H₂O/NPA, 2:3 H₂O/IPA, 2:3 H₂O/TB, 2:1:2 H₂O/NPA/TB and 1:1:3 H₂O/NPA/TB. The specifications of the inks are presented in Table 3.1.

Table 3.1. Specifications of the inks investigated.

Ink	Solvent matrix (w/w)	Approximate dielectric constant (ϵ)	Ultrasonic energy input (kWs)	Roller shaker (days)	Maturation (days)	Coating thickness (μ m)
1	HEN:221	45,70	20	0	1, 4, 7	50
2	HN:23	43,62	20	0	1, 4, 7	75
3	HI:23	43,62	20	0	1, 4, 7	75
4	HT:23	38,10	20	0	1, 4, 7	75
5	HNT:212	39,94	75	3	1, 4, 7	100, 150
6	HNT:113	26,34	75	3	1, 4, 7	100, 150, 200

3.3 Dispersion

The dispersion of the inks was done by first leaving the ink on a magnetic stirrer overnight before dispersing with an US with an amplitude of 50%. The energy limit set for each sample can be seen in Table 3.1. The oscillation of the sonotrode in the US generates heat so the vial was placed in an ice bath to ensure the ink would not overheat. Ink5 and 6 were dispersed further with the RS. Yttria-stabilised zirconia beads were added, the beads were 2 mm and 4 mm in diameter, and one times the inks weight were added of each bead sizes. The vial was then left on the RS at 70 rpm for three days each. Due to the mechanical strength of the beads, the use of the RS was only done after the US to avoid breaking the sonotrode. After the RS, the ink was poured over into another vial, a magnetic stir bar was added, and the ink was left for maturation on a magnetic stirrer at room temperature. If no RS was used the original vial was put on the magnetic stirrer directly after US.

3.4 Rheological test

The rheological measurements of the inks were done with a Kinexus rotational rheometer from Netzsch. The geometry used was 40 mm in diameter with a 4° angle, and the sample was kept at 25 °C. A solvent trap was used to ensure that the sample would not dry out and was filled with the same matrix as that of the ink. The measurements were recorded and processed in the rSpace software by Netzsch. For the rotational measurements the shear viscosity was recorded for shear rates from 0 to 1000 s⁻¹ and measured at 30 points. For the oscillating measurements, a constant frequency was kept at 1 s⁻¹ while increasing the shear stress logarithmically from 0.01 to 100 Pa, recording five points per decade. Each measurement was run thrice for each sample and the final measurements were used for analysis. Rheological tests were performed on Ink2-4 after seven days of maturation, while for Ink5 and 6 it was performed after one day, four days and seven days of maturation.

3.5 Film application and drying

To produce the CL, the inks were applied onto a decal with a doctor blade and a film applicator. A decal was cut to size and placed with the reinforcing side facing down. The decal was then set into place and a suction was generated to keep the decal flat. The coating thickness was set with the height of the doctor blade, see Table 3.1 for specifications, as well as the speed at which the applicator moved, and the ink was added to the decal. All inks were coated with a coating speed of 75 mm/s and were coated after one day, four days and seven days of maturation. Once the film was applied, the now wet electrode was placed under a plexiglass cover to protect it from dust and other impurities, and left to dry overnight, see Figure 3.1a).

To test how a higher RH impacts the crack formation during drying, a smaller coating sample was placed under a glass cover together with a watch glass containing deionised water. After the coating had dried there was still water left in the watch glass. An image of the set up can be seen in Figure 3.1b). It is important to note that the lower gas volume would not only increase the RH but also the partial pressure of the organic solvents used in the dispersion matrix.

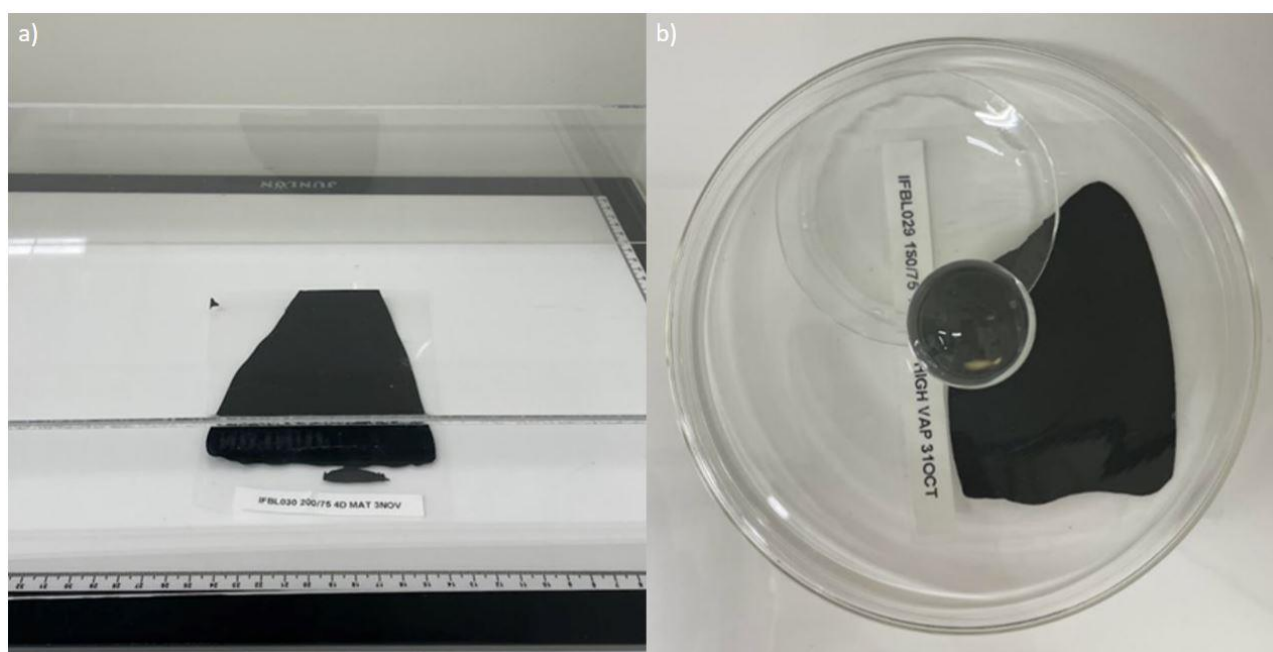


Figure 3.1. Set up for drying under a) normal conditions, and b) at higher RH, watch glass filled with deionised water.

3.6 Light microscopy

Once the coatings had dried the electrodes were visually inspected using a digital microscope (Leica DVM6 A). The digital microscope uses a camera which enables images to be taken easily. The two lenses used had a field of view (FOV) of 3.60 and a FOV of 12.55. Multiple images were taken with varying magnification to evaluate the electrode coatings. Features of interest were the origin of cracks formed, the number and size of the cracks, and any defects that stand out from the bulk of the coating. The cracks were divided into defect cracks, which originate in defects such as aggregates, dust particles and impurities, and stress cracks. The stress cracks were identified as cracks without clear origin, such as aggregates, and thereby assumed to stem from internal stresses in the coating that form during the drying process.

3.7 Scanning electron microscope

The light microscope has some limits, mainly that the smallest objects possible to observe cannot be smaller than the wavelength of the light. While it is not as much of an issue when large defects and cracks are present, it can be hard to get an idea of the porosity and ionomer distribution on the catalyst. Therefore, images were taken with the tabletop SEM at Chalmers Material Analysis Lab. The acceleration voltage was set to 5 kV with a working distance of 7–8 mm, the specifications are stated in each image, and taken with a backscattered electron sensor.

4 Results and discussions

4.1 Dispersion matrix

The results and discussion section has been divided into impacts of the dispersion matrix and the impact of the processing. As mentioned in section 2.2, the choice of dispersion matrix has a significant impact on the resulting electrode coating and the inks rheological behaviour. First, the choice of matrix is discussed based on observations made from the microscope images and the rheological analysis.

4.1.1 HEN:221 inks

Based on previous inks made at PowerCell, the first ink that was investigated had a dispersion matrix with a water to ethanol to NPA weight ratio of 2:2:1. The dispersion matrix has an estimated dielectric constant of 45.70. In Figure 4.1 are the microscope images presented, showing how the electrode quality varies with maturation time.

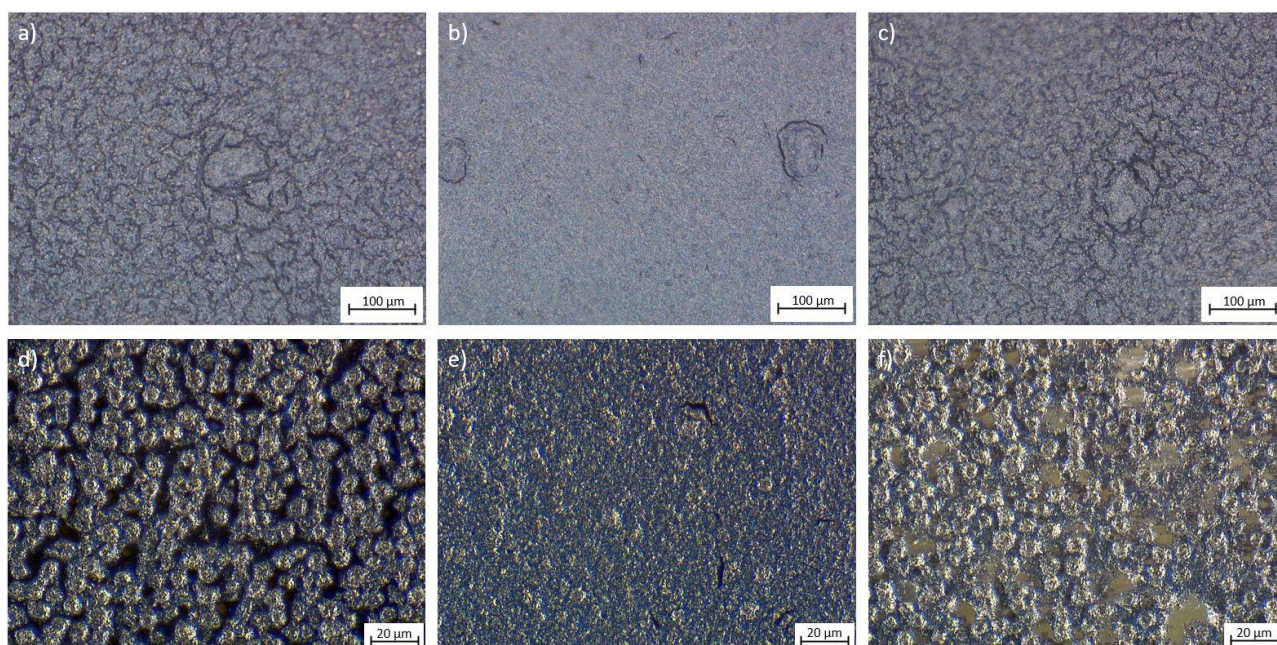


Figure 4.1. Light microscope images of 50 μm coatings of Ink1 on glass fibre reinforced decal. a) and d) are taken after one day of maturation, b) and e) after four days of maturation, and c) and f) after seven days of maturation. a), b), and c) are taken with maximum magnification with a FOV 12.55 lens and has a scale bar of 100 μm , while d), e) and f) are taken with maximum magnification with a FO V3.6 lens and has a scale bar of 20 μm .

The features to look for when assessing a coatings quality are the number of cracks and their size, their origin, any aggregates, and whether the aggregates cause cracks. Though the cracks make it harder to identify aggregates, some larger ones can be seen in Figure 4.1a-c). The aggregates are visible as they stand out from the bulk. Their presence changes the cracking behaviour, causing cracks in Figure 4.1b), and they indicate that the dispersion step of the process needs further development. The aggregates could be removed by having a higher energy input during US or adding an additional dispersing step with the RS. These aggregates highlight the necessity of a thorough dispersion to make all the catalyst available and to avoid crack formation, and to increase durability.

As seen in Figure 4.1, the coating quality changes dramatically with maturation time. From images with higher magnification in Figure 4.1d) and 4.1f), a ball-like structure seems to be a

cause of the crackly structure. The change in quality over time suggests that during maturation there is a change in the interactions between compounds of the ink. It could be that the long side-chained ionomers need the time to create a stronger interaction with the catalyst particles which would stabilise the catalyst particles. The stabilisation would both come from the steric hinderance from the ionomers and the electrostatic repulsion between the sulphonic groups on the sidechains. The catalyst tends to form aggregates which might cause the large ionomer molecules to need time to move into the pores of these aggregates. Once there, the ionomer could stabilise the catalyst and improve the electrodes cracking behaviour. The worsening of the cracking behaviour after seven days of maturation could be from poor interactions between the hydrophobic HSAC support and the polar dispersion matrix. The poor interaction could cause the catalyst particles to flocculate into larger clusters. If the catalyst flocculate, it could cause the ionomers to move from laying on the surface of the catalyst particles to reform into coils. Whatever the cause, the worsening of the coating quality seen in Figure 4.1f) would suggest that stability of the ink is influences by the maturation step. To try to get a better understanding of the structural changes that happen during maturation in Ink1, SEM images were taken after one day, four days and seven days maturation. These images are presented in Figure 4.2, for a higher resolution of Figure 4.2d)-f) see Appendix.

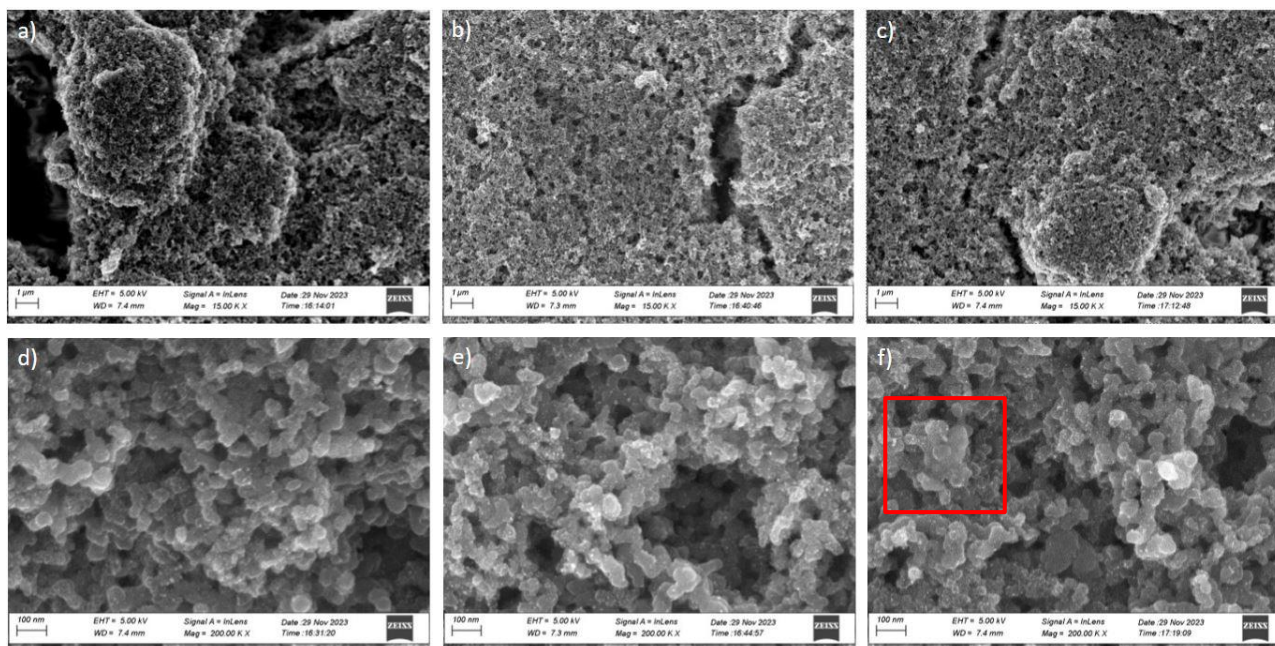


Figure 4.2. SEM images of 50 μm coatings of Ink1 on glass fibre reinforced decal. a) and d) are taken after one day of maturation, b) and e) after four days of maturation, and c) and f) after seven days of maturation. a), b), and c) are taken with $\times 15\,000$ magnification and has a scale bar of 1 μm , while d), e) and f) are taken with $\times 200\,000$ magnification and has a scale bar of 100 nm. Red box in f) highlights a cluster of ionomers covering the HSAC support.

What is evident from Figure 4.2b) is that there are some 1 μm aggregates present in the bulk of the coating. These smaller aggregates indicates that there is either poor interaction between ionomers, catalyst, and dispersion matrix, or that the ink had not been dispersed enough, or both. These smaller aggregates are also present in 4.2c), though less noticeable due to the ball-like structure present. That there are smaller aggregates present in combination with that the coating has a wet thickness of 50 μm means that further development of the ink is needed to get coatings with higher platinum loadings. Also, when comparing the SEM images in Figure 4.2a-c), the porosity of the electrode coating seems to lessen with more maturation time.

When identifying the compounds of the coating in Figure 4.2d-f), the spherical globes of about 50 nm are the HSAC support, they can appear lighter due to charging effects. The platinum on

the HSAC support is a couple of nm in size and can be seen as white spots. The element contrast is due to the higher atomic weight of platinum, resulting in stronger signals from the backscattered electrons. The ionomer is harder to distinguish but can be seen coating the HSAC, making individual particles less visible. A cluster is visible in the red box in Figure 4.2f). Analysing the images becomes sensitive to interpretations because the ionomer is difficult to distinguish from the HSAC support. Comparing Figure 4.2d) and f), the four days maturation sample shows less ionomer clusters and more platinum particles, and a more even distribution of the platinum particles. That the platinum signal is visible through the ionomer coating could indicate a thinner ionomer coating for the four days of maturation sample. A thinner ionomer coating could be because the catalyst particles are more dispersed making less ionomer available to cover each particle, compared to the ionomer needed to cover a larger catalyst aggregate. The changes seen from the one day and to the four days maturation samples could be that the ionomer needs time to create a stronger interaction with the catalyst, as mentioned previously. One thing that needs to be taken into consideration though is that these are images of just one small area of the electrodes. More images would be needed to ensure that similar structures are present in all parts of the electrode.

4.1.2 Impact of alcohol on coating quality

Inks with a water to alcohol ratio of 2:3 were prepared to compare the impact of alcohol choice on the resulting electrode. The alcohols explored were NPA, IPA and tert-butanol. Ethanol was excluded due to the high vapour pressure as well as high dielectric constant which was predicted to result in poor ionomer-solvent interactions and fast evaporation and would thereby cause stress cracks.

Rheology tests were conducted on each of the inks (Ink2, Ink3 and Ink4) by the seventh day of maturation and the results are presented in Figure 4.3. From these graphs a higher viscosity was recorded for Ink4 containing tert-butanol, then for Ink3 with IPA and lowest for Ink2 containing NPA. The higher viscosity suggests that the ionomer has a looser structure in the tert-butanol resulting on more entanglements between ionomer molecules. This follows the theory that a lower dielectric constant causes a looser coil of the ionomer. The difference between the IPA and NPA inks can on the other hand not be explained by the dielectric constant alone as it is the same for both solvents. Their viscosity is also the same and can neither explain the observed behaviour. One factor that could explain the behaviour is the molecular structure of the solvents. IPA has a symmetrical structure while NPA has the polar OH-group on one side and the aliphatic hydrocarbon chain on the other side. The asymmetry allows NPA to display weak surfactant-like properties. If it would cause the NPA molecules to arrange around the sulphonic groups, it could weaken the electrostatic repulsion and thus decrease the viscosity. The difference in molecular structure resulting in difference in behaviour has been suggested by Lei et al. [14]. The difference in viscosity is however very small, especially compared to the ink containing TB.

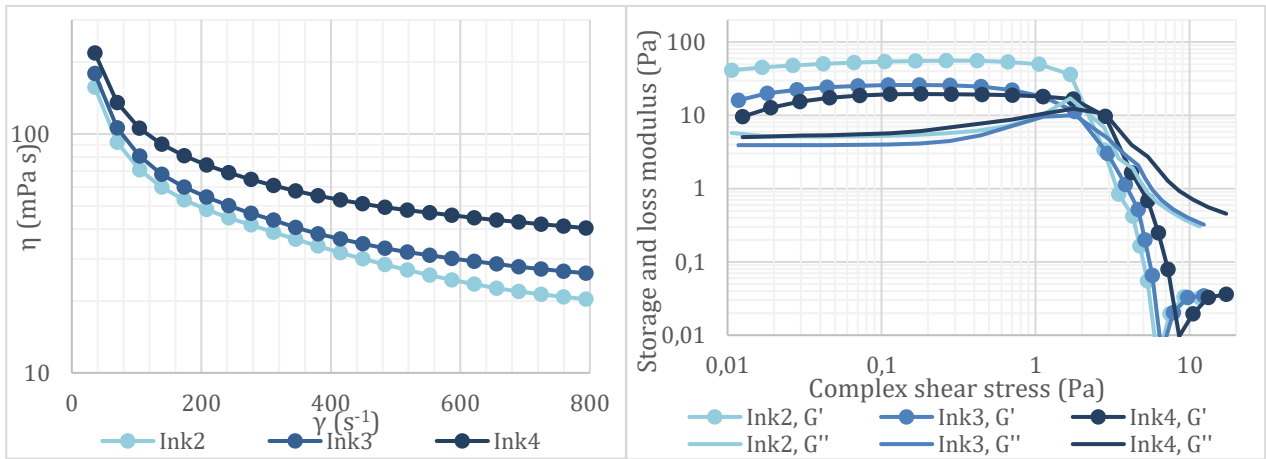


Figure 4.3. Rheology measurements of Ink2 (HN:23) in light blue, Ink3 (HI:23) in blue, and Ink4 (HT:23) in dark blue. The left graph shows rotational viscosity test and right graph show oscillating modulus test.

The results from the oscillation measurements show that the three inks had a similar shear independence with the LVER stopping at a similar shear stress. NPA causes the ink to have a larger magnitude of LVER compared to inks containing TB and IPA. The higher magnitude indicates that the Ink2 has a more elastic response to deformation compared to Ink3 and Ink4. The more elastic response means that the NPA ink is more resistant to deformations when exposed to external shear.

4.1.2.1 NPA inks

Figure 4.4 displays the microscope images of the Ink2 containing a water to NPA ratio of 2:3 taken after one day, four days and seven days of maturation.

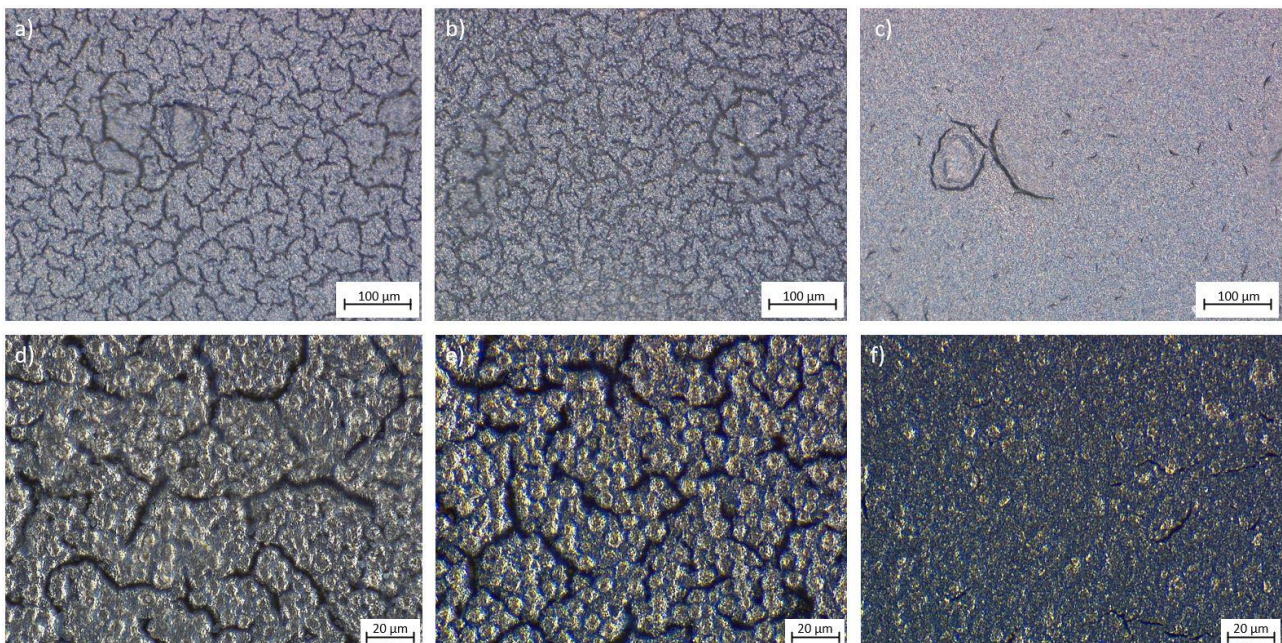


Figure 4.4. Light microscope images of 75 μm coatings of Ink2 on glass fibre reinforced decal. a) and d) are taken after one day of maturation, b) and e) after four days of maturation, and c) and f) after seven days of maturation. a), b), and c) are taken with maximum magnification with a FOV 12.55 lens and has a scale bar of 100 μm , while d), e) and f) are taken with maximum magnification with a FOV 3.6 lens and has a scale bar of 20 μm .

A clear difference between the coatings can be seen where more time of maturation improves the quality of the coatings. As the cracking behaviour seems to be best after seven days of maturation for Ink2, compared to four days for Ink1, it would imply that the optimum

maturation time is dependent on the ink. The worsening of the cracking behaviour seen with Ink1 in Figure 4.4 cannot be seen here. The worsening would not happen if the optimum maturation time was around or after seven days. It would be interesting to see if there is a change in the cracking behaviour after seven days of maturation.

The solvent matrix impacts the optimum maturation time, and it could also impact the stability of the ink. The NPA is less polar than ethanol, which was used in Ink1, and NPA should improve both the ionomer-dispersion matrix interaction, and the catalyst-dispersion matrix interaction. These improved interactions should decrease the drive for phase separations between the compounds and thereby increase the stability of the ink. Again, to confirm this theory the ink would need to be tested after more than seven days of maturation.

4.1.2.2 IPA inks

Figure 4.5 presents the microscope images of the Ink3 containing a water to IPA ratio of 2:3 taken after one day, four days and seven days of maturation.

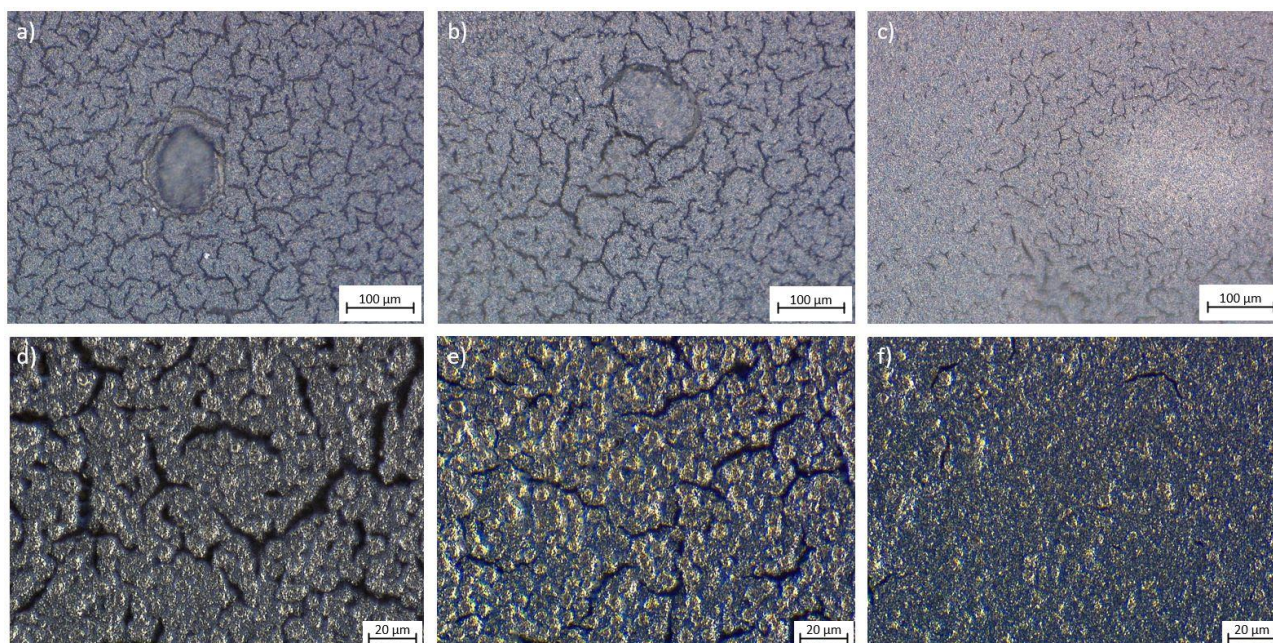


Figure 4.5. Light microscope images of 75 μm coatings of Ink3 on glass fibre reinforced decal. a) and d) are taken after one day of maturation, b) and e) after four days of maturation, and c) and f) after seven days of maturation. a), b), and c) are taken with maximum magnification with a FOV 12.55 lens and has a scale bar of 100 μm , while d), e) and f) are taken with maximum magnification with a FOV 3.6 lens and has a scale bar of 20 μm .

Figure 4.5 illustrates again that maturation seems to improve the cracking behaviour, though the improvement was not as large as that of Ink2 containing NPA. A potential cause for the worsened cracking behaviour between the inks could be the higher vapour pressure of IPA which increases the evaporation rates. Another potential cause could be that the surfactant-like behaviour from NPA's molecular structure enables a better interaction between the ink compounds. The difference in the quality of the coatings from Ink3 compared to the coatings of Ink2 by seven days of maturation is why NPA was chosen over IPA when making tertiary dispersion matrices.

4.1.2.3 TB inks

Presented in Figure 4.6 are the microscope images of the Ink4 containing a water to TB ratio of 2:3 taken after one day, four days and seven days of maturation.

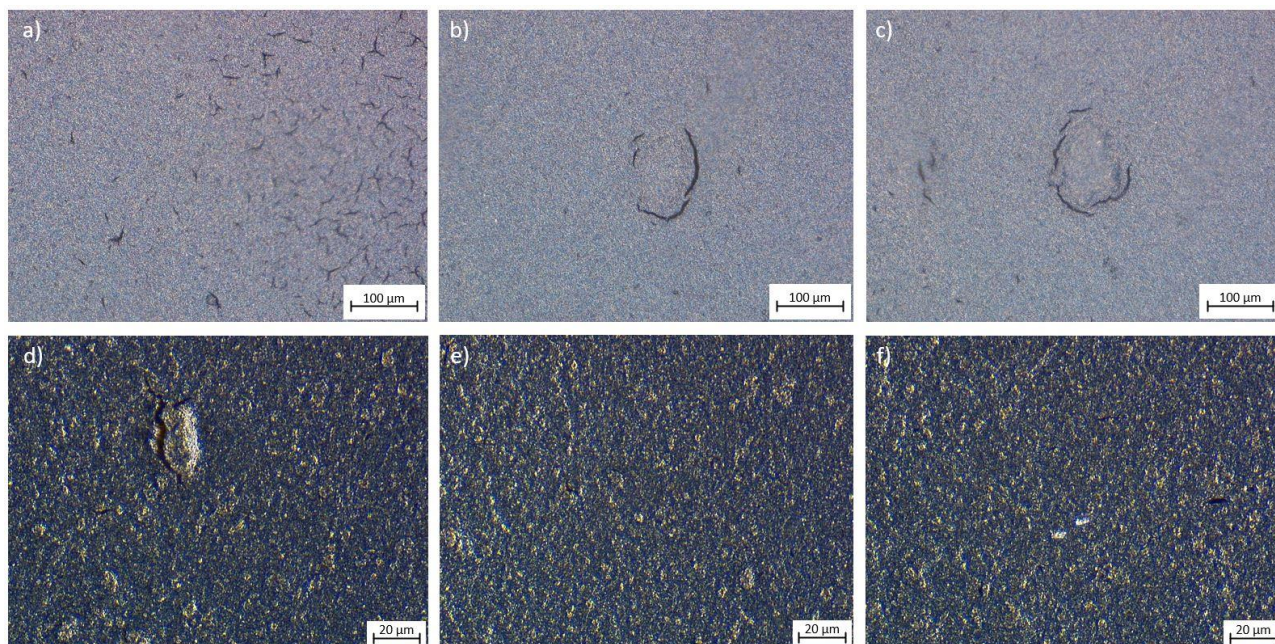


Figure 4.6. Light microscope images of 75 μm coatings of Ink4 on glass fibre reinforced decal. a) and d) are taken after one day of maturation, b) and e) after four days of maturation, and c) and f) after seven days of maturation. a), b), and c) are taken with maximum magnification with a FOV 12.55 lens and has a scale bar of 100 μm , while d), e) and f) are taken with maximum magnification with a FOV 3.6 lens and has a scale bar of 20 μm .

Again, increased maturation time shows an improvement in reducing cracks. The cracking behaviour of Ink4 is largely improved compared to Ink1-3, already after one day of maturation. Thereafter, the difference in cracking behaviour is not as large with more maturation time as that of the inks previously mentioned. The lack of change over different maturation time could be attributed to the low dielectric constant of TB which allows the ionomer to stretch out making the ionomer more available to interact with the catalyst and other ionomers. Therefore, the ink would need less maturation time to create a stronger ionomer-catalyst interaction and could explain why there is little difference between the four and seven days of maturation samples. The lower dielectric constant would also improve the interactions between the HSAC support of the catalyst and the dispersion matrix. There would therefore be a lower driving force for the catalyst particles to flocculate to lessen the interactions.

There is no clear worsening of the cracking behaviour between the coatings with longer maturation time which could mean that the stability of the ink is also improved. If the ionomer is more stretched out, it could better stabilise the catalyst particles and prevent them from flocculating which could be another cause of this improved stability. Not only is the amount of stress crack less with more maturation time, the surface of the coatings also seems more even with fewer smaller aggregates, see Figure 4.6d-f). The smaller aggregates point towards a better catalyst utilisation but would need to be confirmed with more tests.

4.1.3 HNT:212 inks

The results from the impact of the alcohol choice suggests that the next step would be to explore how combining alcohols would impact the inks behaviour. The alcohols selected were NPA, due to its low vapour pressure, and TB, due to its low dielectric constant. The dispersion matrices chosen had a water to NPA to TB ratio of 2:1:2 (Ink5) and 1:1:3 (Ink6) with the first having a higher dielectric constant due to having more water. Determining how the different solvents would evaporate is not as clear due to a tertiary solvent system being much more complex than

a binary system. This complexity is also not accounting for interactions between the solvents and the ionomer and the catalyst. It could stand to reason that the TB would be the first solvent to evaporate due to the higher vapour pressure, see Table 2.1. As seen in the coatings made with Ink1, 2, 3 and 4, there were still aggregates present after US which is why the energy input was increased for Ink5 and 6, see Table 3.1. Ink5 and 6 were also dispersed with the RS for three days to grind down any remaining aggregates. An improved cracking behaviour was expected so the coatings' wet thickness was increased to 150 μm . The thicker coating would result in a higher platinum loading. Presented in Figure 4.7 are the light microscope images of the Ink5 containing a water to NPA to TB ratio of 2:1:2 taken after one, four and seven days of maturation.

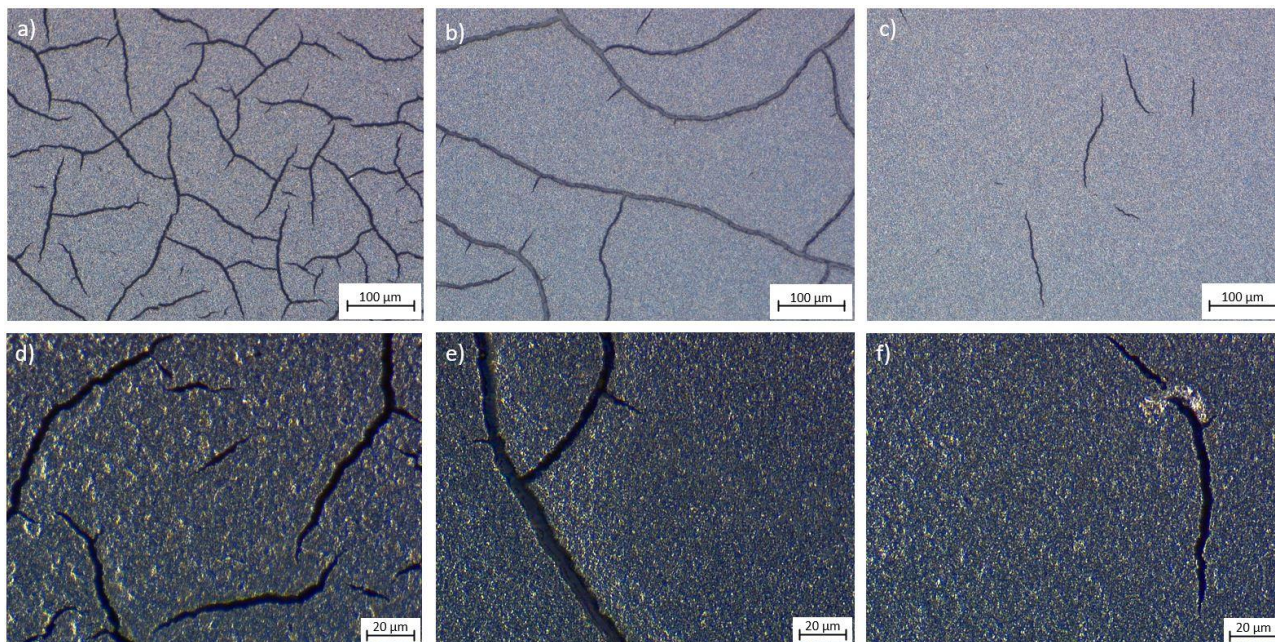


Figure 4.7. Light microscope images of 150 μm coatings of Ink5 on PET reinforced decal. a) and d) are taken after one day of maturation, b) and e) after four days of maturation, and c) and f) after seven days of maturation. a), b), and c) are taken with maximum magnification with a FOV 12.55 lens and has a scale bar of 100 μm , while d), e) and f) are taken with maximum magnification with a FOV 3.6 lens and has a scale bar of 20 μm .

Just as for Ink1-4, there is an improvement in cracking behaviour with maturation time. The coating after one day of maturation has many cracks though they are less in number than that of Ink1, 2 and 3. The ball-like structures are also not as clear. The improved cracking behaviour and the more even structure could mean that, as predicted, the presence of the TB helps the ionomer to form interactions with the catalyst particles. It was not possible to explore the cracking behaviour for longer maturation than seven days so it would be interesting to see if the behaviour improved further with more time, or if the optimum maturation time had been reached. There is a difference in the surface structure in Figure 4.7d)-f), and SEM images were taken of the three coatings to get a closer look said differences. In Figure 4.8 these SEM images are presented, for a higher resolution of Figure 4.7c) and d) see Appendix. Unfortunately, it was not possible to take images of the four days maturation sample as it showed charging effects over the entire sample. The charging effects points towards poor interactions with the decal it was coated onto which could indicate poor durability. Parts of the coating also flaked off when the sample was cut to fit in the SEM which further points to poor interaction with the decal.

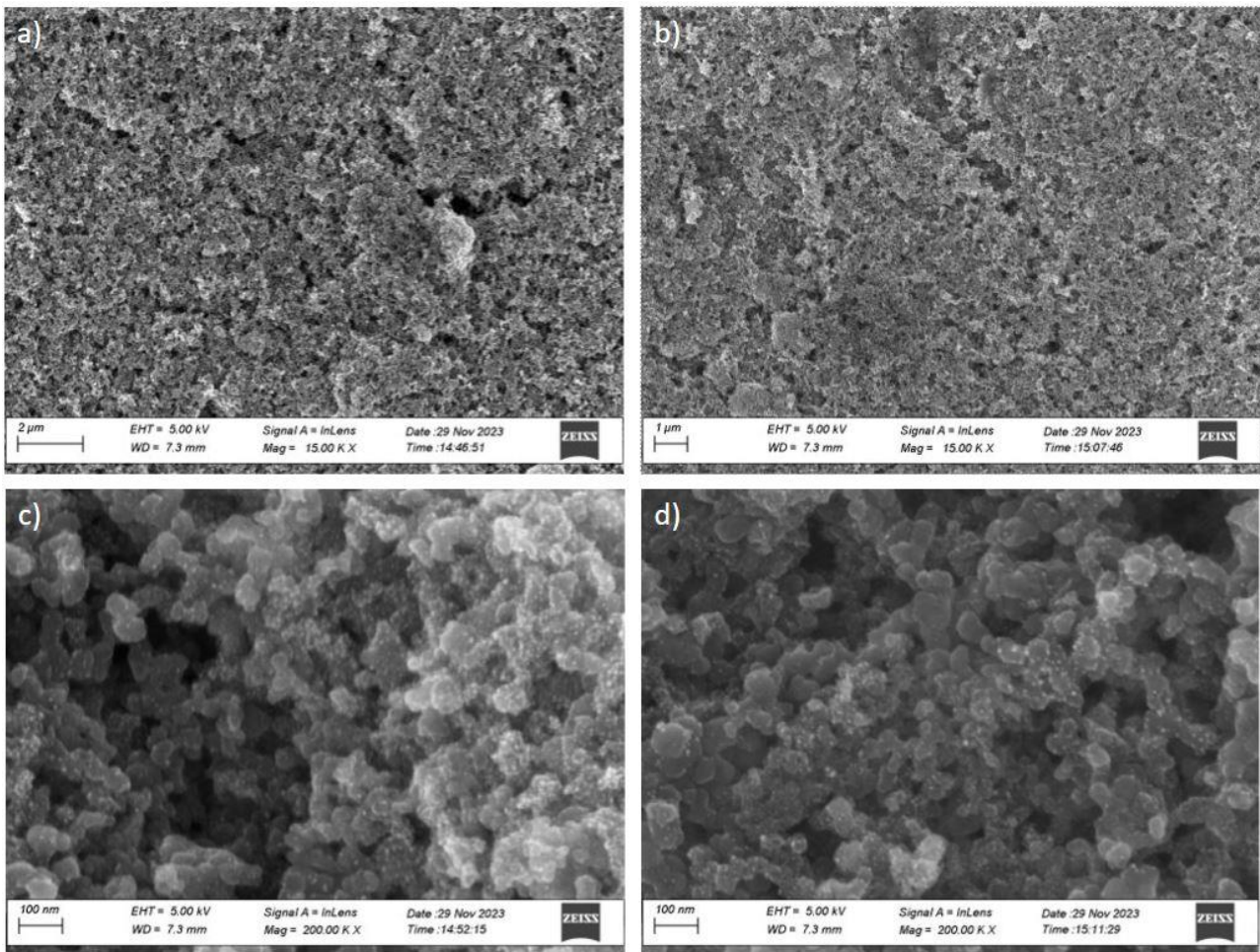


Figure 4.8. SEM images of 150 μm coatings of Ink5 on PET reinforced decal. a) and d) are taken after one day of maturation, and b) and d) after seven days of maturation. a) and b) are taken with $\times 15\,000$ magnification and has a scale bar of 1 μm , while c) and d) are taken with $\times 200\,000$ magnification and has a scale bar of 100 nm.

Comparing the SEM images in Figure 4.8 there is little difference between the samples. The coating in Figure 4.8a) seem slightly less even but more porous than 4.8b). Figure 4.8a) also show more prominent aggregates. The less even coating is reasonable as more aggregates would cause less material to be available in the bulk coating and result in more stresses. The porosity of the CL is an important factor regarding the performance of the electrode in a fuel cell. A less porous layer would increase the gas transport resistance making it harder for oxygen to reach the platinum to react. To further investigate the change in the inks' behaviour, rotational and oscillating rheological tests were performed on Ink5. Figure 4.9 shows the change in viscosity and the modulus properties after one day, four days and seven days of maturation.

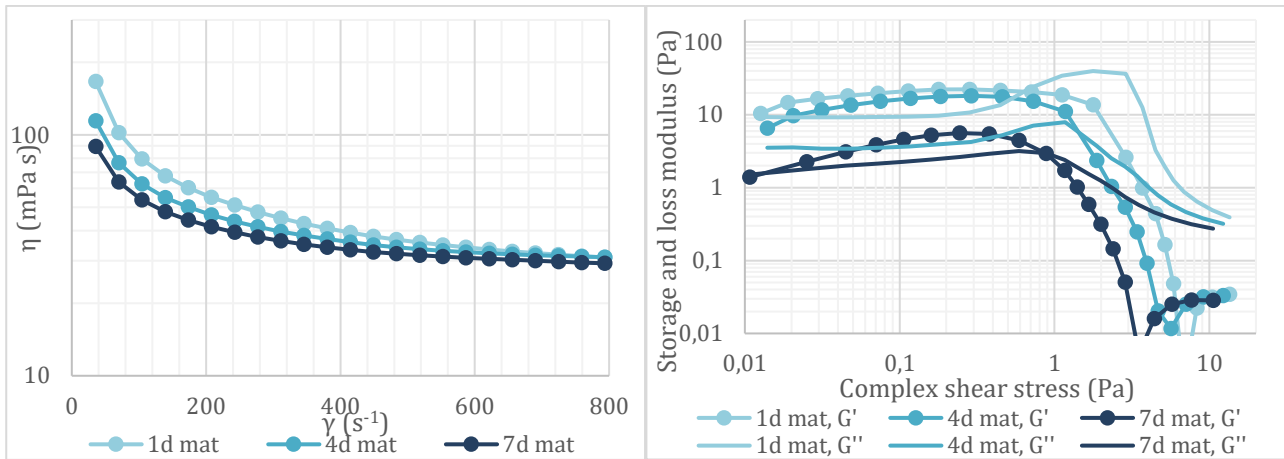


Figure 4.9. Rheology measurements of Ink5 (HNT:212) over different maturation times, one day of maturation in light blue, four days of maturation in blue, and seven days of maturation in dark blue. The left graph shows rotational viscosity test, the right graph shows oscillating modulus test with dot-marked lines indicating the storage modulus (G') while unmarked lines indicate the loss modulus (G'').

The decrease in viscosity with more maturation could be the result of an increased interaction between the ionomer and catalyst. Increased interactions would mean that there is less free ionomer left to entangle, and that the effective volume fraction of the particles would decrease and thereby lower the viscosity. It could also be that the ionomer has time to move into the mesopores between the catalyst particles that form submicron aggregates. If more of the ionomer is situated in the mesopores it would make less ionomer free to interact with each other causing less electrostatic repulsion and less steric hinderance and thereby lower the effective radius of the particles.

4.1.3.1 Higher relative humidity during drying

To explore how the drying conditions impact the electrodes quality, two coatings of Ink5 were left to dry under different conditions. One was kept under a plexiglass cover, see Figure 3.1a), while the other dried with the setup show in Figure 3.1b) to increase the relative humidity. The microscope images of the two coatings are presented in Figure 4.10, and they were coated after one day of maturation.

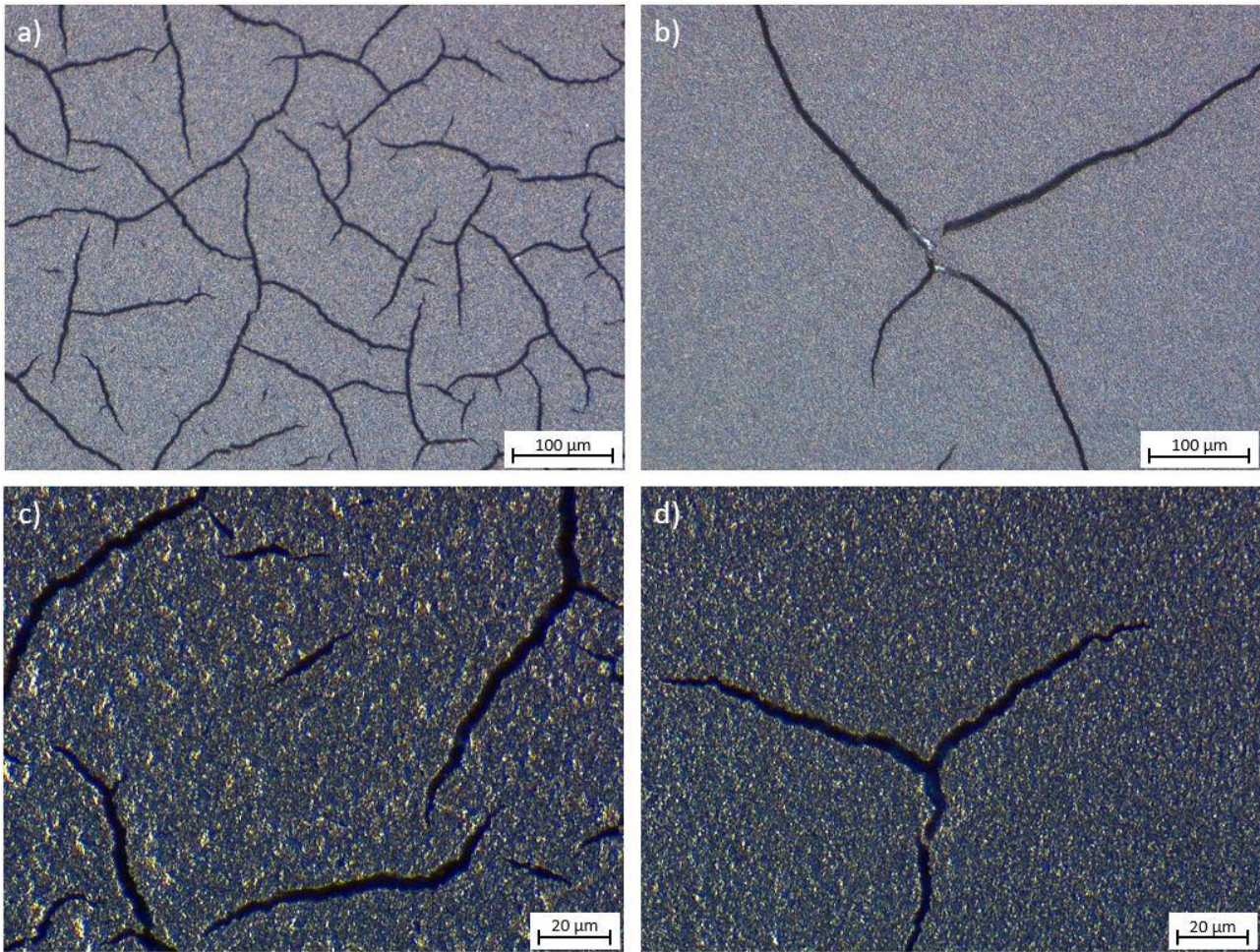


Figure 4.10. Light microscope images of 150 μm coatings of Ink5 on PET reinforced decal after one day of maturation. a) and c) are taken of a coating dried under normal drying conditions, b) and d) are of coatings dried with a set up for increasing RH, see Figure 3.1. a) and b) are taken with maximum magnification with a FOV 12.55 lens and has a scale bar of 100 μm , while c) and d) are taken with maximum magnification with a FOV 3.6 lens and has a scale bar of 20 μm .

As seen in Figure 4.10, changing the drying conditions have a significant impact on the resulting coating. The results follow previous results found at PowerCell where the alcohol used in the dispersion matrix was left in a beaker to evaporate instead of water [8]. It seems like in neither sample in Figure 4.10 did the cracks originate from any imperfections and are therefore classified as stress cracks. The reason for the diminished number of cracks could be due to the higher RH causing the solvents to evaporate slower, giving time for the ink compounds to rearrange. Therefore, less stress is formed in the coating, resulting in fewer cracks. Something that needs to be taken into consideration is putting the smaller cover over the coating would also increase the partial pressure of the alcohols. Increasing the vapour pressure for all the solvents in the ink would improve crack formation as well. Which RH result in least cracking was not investigated further but it highlights how the drying process can be used to control crack formations.

4.1.4 HNT:113 inks

Continuing with the HNT inks, figure 4.11 presents the light microscope images of the Ink6 containing a water to NPA to TB ratio of 1:1:3 taken after different days of maturation.

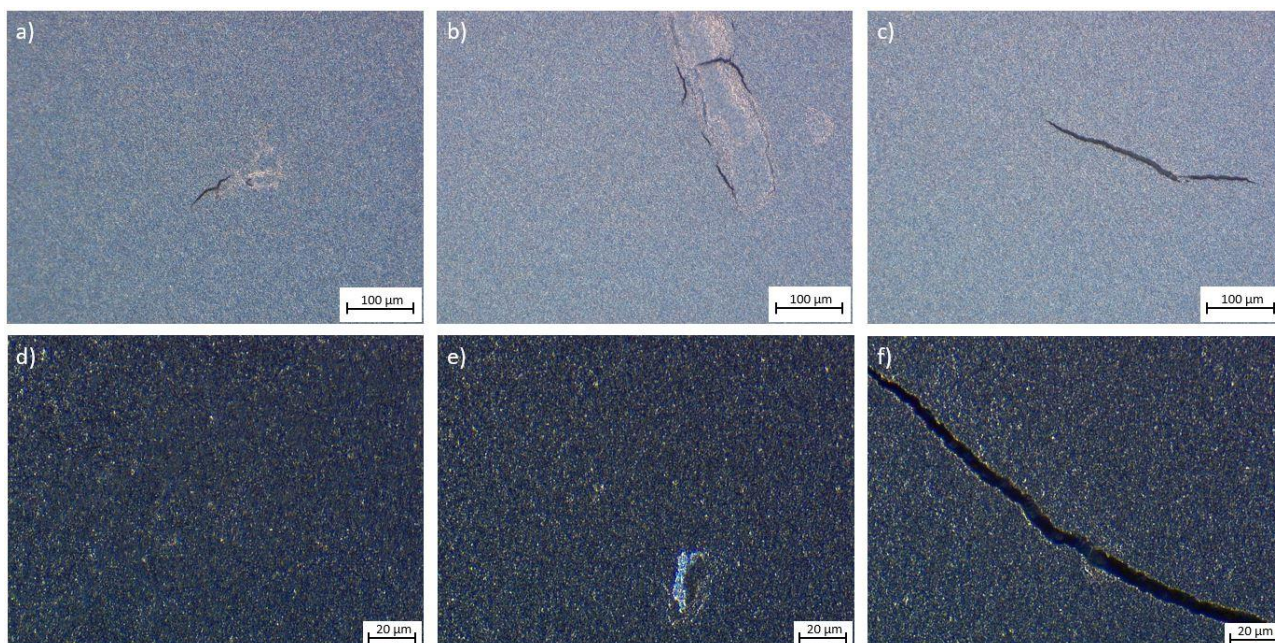


Figure 4.11. Light microscope images of 150 μm coatings of Ink6 on PET reinforced decal. a) and d) are taken after one day of maturation, b) and e) after four days of maturation, and c) and f) after seven days of maturation. a), b), and c) are taken with maximum magnification with a FOV 12.55 lens and has a scale bar of 100 μm , while d), e) and f) are taken with maximum magnification with a FOV 3.6 lens and has a scale bar of 20 μm .

From Figure 4.11 the structure of the coatings has greatly improved compared to those of Ink5 pointing towards improved interactions between the ink's compounds. The cracking behaviour in Figure 4.11 seems to neither improve nor worsen with maturation time. The dispersion matrix seems to help stabilise the ink which could mean that the ionomers have a looser structure that keeps the catalyst particles from flocculating. The lower dielectric constant would also improve the interaction between the matrix and the HSAC support, meaning that the catalyst particles have a lesser driving force to flocculate.

While the bulk of the coatings are crack-free, the cracks still present has origins in imperfections or aggregates. Some, like the one seen in Figure 4.11f), looks like undispersed catalyst which point towards that the dispersion method needs further refining. Others, like the one in Figure 4.11b), has a slightly different shape which, from experience, points towards external imperfections, and in turn highlights the need for a clean working environment. Whether it is dust that has been coated over, or dried ink from the vial walls which has fallen into the ink during the process again is hard to tell. It could also be undispersed catalyst, but it could only for certain be determined through an elemental analysis of the imperfection. The imperfection in Figure 4.11e) shows where a piece of the CL has detached from the decal. Rheological tests were performed on Ink6 to get a more complete view of the impact of maturation time. The results can be seen in Figure 4.12.

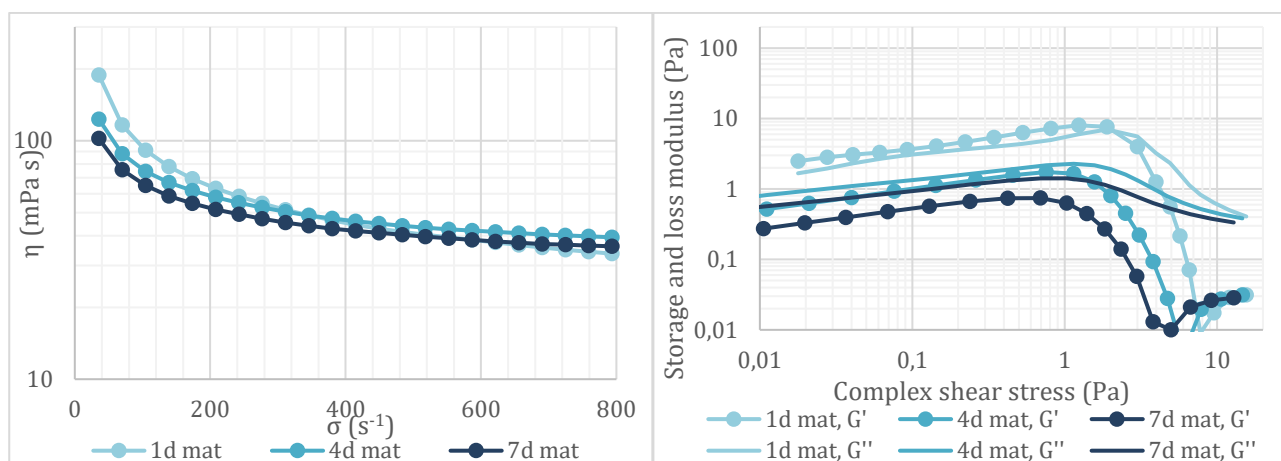


Figure 4.12. Rheology measurements of Ink6 (HNT:113) over different maturation times, one day of maturation in light blue, four days of maturation in blue, and seven days of maturation in dark blue. The left graph shows rotational viscosity test, the right graph shows oscillating modulus test with dot-marked lines indicating the storage modulus (G') while unmarked lines indicate the loss modulus (G'').

Overall, the change in rheological behaviour is small, and just as for Ink5 there is a decrease in viscosity with more maturation time. The decrease in viscosity suggests that more maturation time allows more ionomer-catalyst interactions to form and in turn make less sulphonic groups available to cause electrostatic repulsions. There is a decrease in both moduli, just as for Ink5, but the decrease in storage modulus is substantially larger than that of the loss modulus, which is unlike Ink5. This change in moduli results in a lower storage modulus than loss modulus after four and seven days of maturation. It means that the ink has become viscous dominant, making it less able to retain its shape if exposed to external shear. The LVER also ends at lower shear stress with more maturation time. This means that less stress is needed to start impacting the internal structure of the ink. As stated in section 2.4, the correlations between change in modulus and a change in the inks structure are not well described. The rheological results show that there are structural changes in the ink with more maturation time, even though there are no clear visual changes in the coating. It would be interesting to see how these changes affect the electrochemical properties of the electrodes.

4.1.4.1 Higher relative humidity during drying

Just as for Ink5, to explore how the drying conditions impact the electrodes quality, two coatings of Ink6 were left to dry under different conditions. One was kept under a plexiglass cover, see Figure 3.1a), while the other dried with the setup shown in Figure 3.1b) to increase the relative humidity. The microscope images of the two coatings are presented in Figure 4.10, and they were coated after four days of maturation.

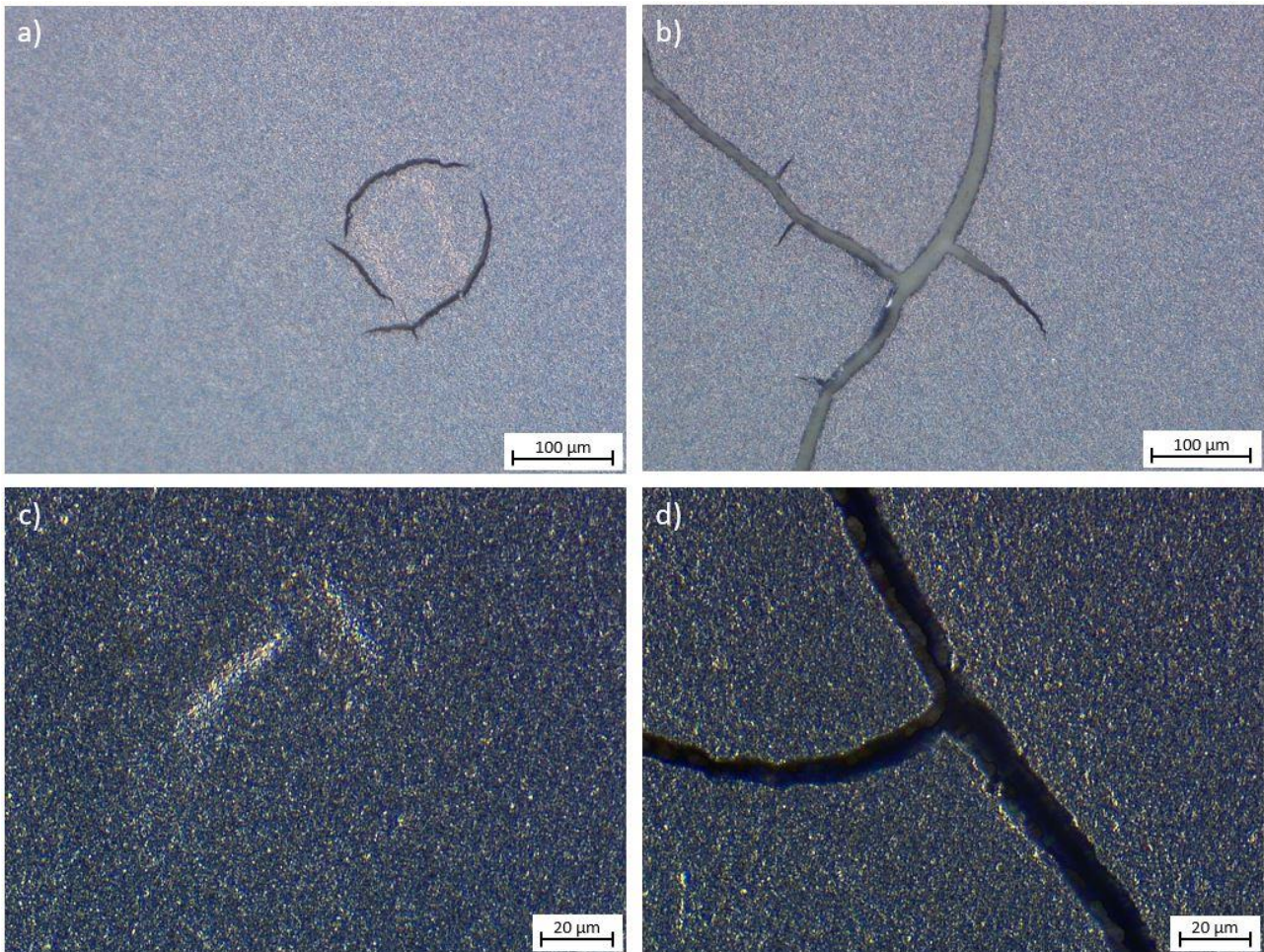


Figure 4.13. Microscope images of 200 μm coatings of Ink6 on PET reinforced decal after four days of maturation. a) and c) are taken of a coating dried under normal drying conditions, b) and d) are of coatings dried with a set up for increasing RH, see Figure 3.1. a) and b) are taken with maximum magnification with a FOV 12.55 lens and has a scale bar of 100 μm , while c) and d) are taken with maximum magnification with a FOV 3.6 lens and has a scale bar of 20 μm .

For Ink6 there is a worsened cracking behaviour when the coatings are allowed to dry with an increased RH, unlike Ink5 which saw an improvement. The difference in behaviour could be due to the changes in the environment around the ionomer during the drying process. Having less water and more TB present in the dispersion matrix could cause the ionomers to initially stretch out more. A higher RH would discourage the water in the ink from evaporating and cause the coating to get a higher water content compared to the other solvents as the coating dries. The increased water concentration could cause the ionomer to form tighter coils, resulting in less interactions to counteract the stresses in the coating during drying. A couple of things that need to be taken into consideration is that the wet thickness here is 200 μm instead of 150 μm which was used for Ink5, and a thicker coating tends to cause more cracking. Another thing to consider is that these coatings were made after four days of maturation instead of one, though from Figure 4.11 there seem to be little difference between one day and four days of maturation for Ink6. The difference in cracking behaviour with higher RH during drying for Ink5 and Ink6 indicates the need for ink-specific drying processes.

4.2 Processing of the inks

During the electrode-making process there are several steps that impact the resulting electrodes in different ways. To see how each processing step impact, electrode coatings were made of Ink5 and Ink6 just after the US step and after the inks had been on the RS for three days. These are compared to coatings from the inks after they were left for one day of maturation and the resulting coatings be seen in Figure 4.14 for Ink5 and Figure 4.15 for Ink6.

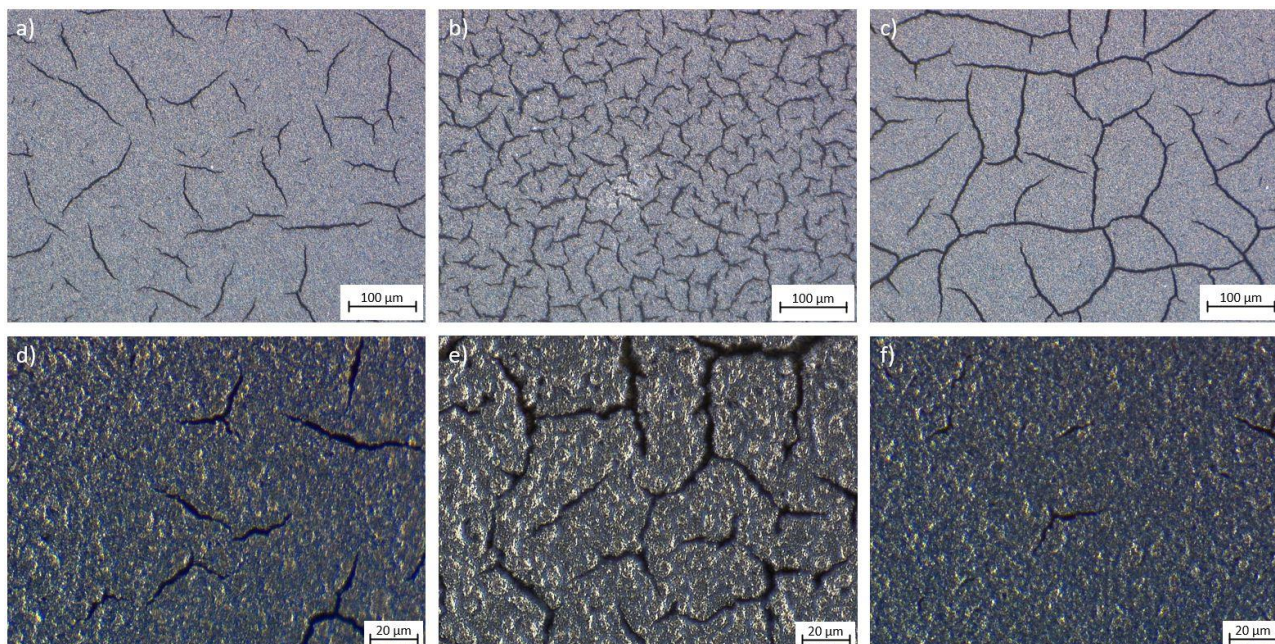


Figure 4.14. Light microscope images of 100 μm coatings of Ink5 on PET reinforced decal. a) and d) are taken after directly after US, b) and e) after three days on RS, and c) and f) after one days of maturation. a), b), and c) are taken with maximum magnification with a FOV 12.55 lens and has a scale bar of 100 μm , while d), e) and f) are taken with maximum magnification with a FOV 3.6 lens and has a scale bar of 20 μm .

For Ink5 there is a clear difference in the resulting cracking behaviour after each processing step. The ink seems well dispersed after the US as seen in Figure 4.14a) and d), while the RS seem to promote crack formation, see Figure 4.14b) and e). From figure 4.14c) and f), the cracking behaviour is improved after one day of maturation. During both the RS and the maturation steps the inks are exposed to shear, though the RS is higher than that of the magnetic stirrer during maturation. It could be that the higher shear does not allow the ionomer to form strong interactions with the catalyst, making the ionomer less available to stabilise the catalyst particles. From these images it seems like the RS step might not be needed for Ink5. It would be interesting to see if the maturation time needed to get an optimal coating would change if the RS was excluded from the process.

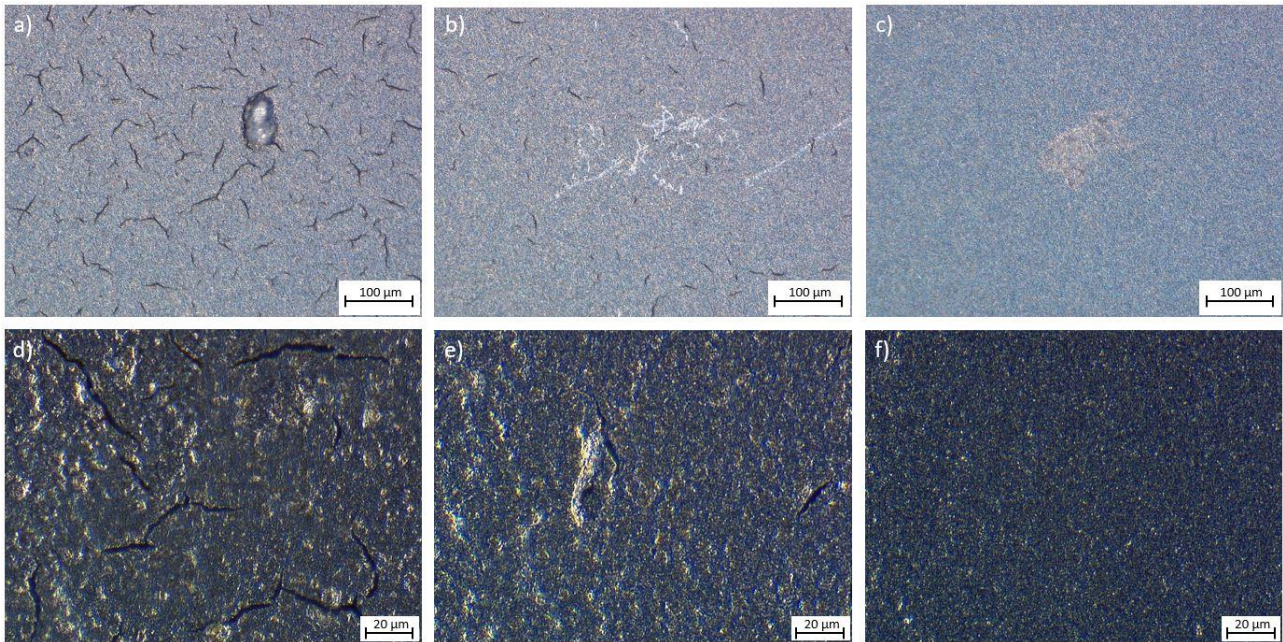


Figure 4.15. Light microscope images of 100 μm coatings of Ink5 on PET reinforced decal. a) and d) are taken directly after US, b) and e) after three days on RS, and c) and f) after one days of maturation. a), b), and c) are taken with maximum magnification with a FOV 12.55 lens and has a scale bar of 100 μm , while d), e) and f) are taken with maximum magnification with a FOV 3.6 lens and has a scale bar of 20 μm .

From the images in Figure 4.15 it can be seen how the cracking behaviour improves with each step of the process. Figure 4.15a) illustrates the undispersed catalyst aggregates present and indicate the need for further dispersion. Why the US might be enough for Ink5 and not for Ink6 could be attributed to a higher viscosity of Ink6. The higher viscosity means that the energy spreads less throughout the dispersion and that more energy input is needed to get the same result in Ink6 as in Ink5. After the RS less aggregates are present and from Figure 4.15d)-f) the surface of the coating seems more even after the RS. Noteworthy is that the scratches seen in Figure 4.15b) are from removing the electrode from the zip-lock bag the dried coatings were stored in. Overall, there was little difference between the cracks present in the coatings in Figure 4.11. It does however show having at least one day of maturation after RS improves the cracking behaviour. It also seems to make the surface more even which could be attributed to the lower shear of the magnetic stirrer allows interactions between the ink compounds to form.

Conclusion

This work set out to find factors that impact the ink used for prototyping electrodes for PEMFC. The work was based on catalyst inks with different dispersion matrices, rheological analysis of the inks and visual analysis of the resulting electrodes. To evaluate the quality visually, the main features explored were crack formation and the size and number of aggregates. When it comes to the dispersion matrix, important properties were found to be the dielectric constant and vapour pressure of its compounds. Dispersion matrices with a lower dielectric constant resulted in more even coatings and higher viscosities of the inks, specifically for Ink4 and Ink6. These observations indicate that a lower dielectric constant improves the interactions between the ionomer, the catalyst, and the dispersion matrix. The improvement seen with compounds having a lower vapour pressure could be because it slows down the drying of the coatings. The slower drying result in less stress during drying which is visible through less stress cracks in the coatings. This difference can be seen when comparing Ink2 which contained IPA, with Ink3 which contained NPA. These two properties do not give a full image of the quality and performance of the electrodes, but they should be taken into consideration when choosing which matrix to start exploring.

During the experiments, maturation was seen to have a large impact on all the inks and their electrode's quality. Leaving the samples on the magnetic stirrer for up to seven days significantly changed the quality from an unacceptable number of cracks to much fewer cracks as seen for Ink5. While the exact mechanism is unknown some theories has been proposed. Rheological analysis showed a decrease in viscosity, and storage and loss modulus with more maturation time indicating improved interactions between the compounds of the ink. The need for longer maturation time may be attributed to that the ionomer needs time to disperse into the mesopores of the catalyst and provide both steric and electrostatic stabilisation. The stabilisation would help prevent the catalyst particles from flocculating. Having more dispersed compounds would lead to more individual catalyst particles being covered by ionomer. There would be less the free ionomer available to interact which would both lower the electrostatic repulsion and making less ionomers available to entangle. The amount of time each ink needs for maturation seem to be individual and connected to the interaction between the ink compounds. The interactions between the compounds could partly be explained by the dielectric constant of the dispersion matrix. The findings indicate that too much time can have a negative impact on the quality and should therefore be explored further for each ink. Further analysis is needed to validate the theories presented in this work.

While not a main focus for this study, the conditions during drying was found to have a large impact on the crack formation. The impact can be both positive, lessening the number of cracks, and negative, worsening the number of cracks. The optimal drying conditions can therefore also be seen as individual to each ink and can be used as a tool to control the crack formation and propagation.

Outlook

There is very little research that has been done to investigate what happens during maturation. This work indicates it could be a factor for future investigations when designing electrodes for different purposes. It would be interesting to investigate both the changes in structure in the inks and any potential reactions happening in the ink. By understanding what happens during this stage, predictions could potentially be made as to how long maturation time is optimal for an ink's stability and how to scale up the production of electrodes.

The ink's behaviour is individual to each composition. It is therefore important find the optimal dispersion method, maturation time and drying conditions to get the best suited electrode quality. During this study each ink was only made once so an extensive statistical analysis would therefore be needed to determine the accuracy and precision of this work. It would also be needed to set some of the limits regarding the stability of an ink.

As you have seen in this paper, along with numerous others, the choice in dispersion matrix impacts the structure and cracking behaviour of the electrode coating. It can give some insight into the durability of the electrode, but understanding how the choice impact the electrochemical behaviour needs to be further investigated. Aside from putting the coatings into a cell, investigating the electrodes porosity and oxygen permeability would also give insight into how the choice of dispersion matrix influences transporting reactants. The impact on the transport of reactants would influence the performance of the cell and should therefore be explored.

References

- [1] J. A. Appleby, "Fuel Cell," AccessScience. Accessed: Jun. 07, 2023. [Online]. Available: <https://www.accessscience.com/content/article/a274100>
- [2] PowerCell Group AB, "Services." Accessed: Dec. 15, 2023. [Online]. Available: <https://powercellgroup.com/segments/services/>
- [3] Encyclopædia Britannica, "Fuel cell," Britannica Academic.
- [4] International Energy Agency, "Global Hydrogen Review 2022," 2022. [Online]. Available: www.iea.org/t&c/
- [5] Encyclopaedia Britannica, "Platinum," *Encyclopedia Britannica*. 2023. Accessed: Dec. 15, 2023. [Online]. Available: <https://www.britannica.com/science/platinum>
- [6] N. Malmquist, "Rheological behavior of ionomer dispersions and their incorporation in catalytic inks for use in PEMFC electrodes," Physics, Gothenburg, 2023. Accessed: Dec. 15, 2023. [Online]. Available: <https://odr.chalmers.se/items/1417b260-fa08-4a97-824a-0f7a2774fa76>
- [7] E. Ulberstad, "Investigation of catalyst structure and dispersion methodology on PEMFC catalytic inks and resulting electrodes," Physics, Gothenburg, 2023. Accessed: Dec. 15, 2023. [Online]. Available: <https://odr.chalmers.se/items/3f800814-a972-4887-b7ae-d90ca0dd262e>
- [8] S. Jayaprakash Nair, "Investigation of the influence of coating and drying methods of catalytic inks on the structure of resulting electrodes for PEMFCs," Chalmers University of Technology, Gothenburg, 2024. Manuscript in preparation.
- [9] H. Liu, L. Ney, N. Zamel, and X. Li, "Effect of Catalyst Ink and Formation Process on the Multiscale Structure of Catalyst Layers in PEM Fuel Cells," *Applied Sciences*, vol. 12, no. 8, p. 3776, Apr. 2022, doi: 10.3390/app12083776.
- [10] J.-H. Park, M.-S. Shin, and J.-S. Park, "Effect of dispersing solvents for ionomers on the performance and durability of catalyst layers in proton exchange membrane fuel cells," *Electrochim Acta*, vol. 391, p. 138971, Sep. 2021, doi: 10.1016/j.electacta.2021.138971.
- [11] J. H. Lee, G. Doo, S. H. Kwon, S. Choi, H.-T. Kim, and S. G. Lee, "Dispersion-Solvent Control of Ionomer Aggregation in a Polymer Electrolyte Membrane Fuel Cell," *Sci Rep*, vol. 8, no. 1, p. 10739, Jul. 2018, doi: 10.1038/s41598-018-28779-y.
- [12] A. Tarokh, K. Karan, and S. Ponnurangam, "Atomistic MD Study of Nafion Dispersions: Role of Solvent and Counterion in the Aggregate Structure, Ionic Clustering, and Acid Dissociation," *Macromolecules*, vol. 53, no. 1, pp. 288–301, Jan. 2020, doi: 10.1021/acs.macromol.9b01663.
- [13] T. Nagai and S. Prakongpan, "Solubility of acetaminophen in cosolvents.," *Chem Pharm Bull (Tokyo)*, vol. 32, no. 1, pp. 340–343, 1984, doi: 10.1248/cpb.32.340.
- [14] C. Lei *et al.*, "Impact of Catalyst Ink Dispersing Solvent on PEM Fuel Cell Performance and Durability," *J Electrochem Soc*, vol. 168, no. 4, p. 044517, Apr. 2021, doi: 10.1149/1945-7111/abf2b0.
- [15] S. Du, W. Li, H. Wu, P.-Y. Abel Chuang, M. Pan, and P.-C. Sui, "Effects of ionomer and dispersion methods on rheological behavior of proton exchange membrane fuel cell catalyst layer ink," *Int J Hydrogen Energy*, vol. 45, no. 53, pp. 29430–29441, Oct. 2020, doi: 10.1016/j.ijhydene.2020.07.241.
- [16] S. Khandavalli *et al.*, "Rheological Investigation on the Microstructure of Fuel Cell Catalyst Inks," *ACS Appl Mater Interfaces*, vol. 10, no. 50, pp. 43610–43622, Dec. 2018, doi: 10.1021/acsami.8b15039.
- [17] B. G. Pollet, "The use of ultrasound for the fabrication of fuel cell materials," *Int J Hydrogen Energy*, vol. 35, no. 21, pp. 11986–12004, Nov. 2010, doi: 10.1016/j.ijhydene.2010.08.021.

- [18] H. M. & M. Co. , Ltd. Chemtech Division, "Bead Mill – Grinding & Dispersing."
- [19] C. M. Baez-Cotto *et al.*, "The effect of ink ball milling time on interparticle interactions and ink microstructure and their influence on crack formation in rod-coated catalyst layers," *J Power Sources*, vol. 583, p. 233567, Nov. 2023, doi: 10.1016/j.jpowsour.2023.233567.
- [20] P. Liu, D. Yang, B. Li, C. Zhang, and P. Ming, "Influence of Degassing Treatment on the Ink Properties and Performance of Proton Exchange Membrane Fuel Cells," *Membranes (Basel)*, vol. 12, no. 5, p. 541, May 2022, doi: 10.3390/membranes12050541.
- [21] N. Willenbacher and K. Georgieva, "Rheology of Disperse Systems," in *Product Design and Engineering*, Wiley, 2013, pp. 7–49. doi: 10.1002/9783527654741.ch1.
- [22] D. I. Wilson, "What is rheology?," *Eye*, vol. 32, no. 2, pp. 179–183, Feb. 2018, doi: 10.1038/eye.2017.267.
- [23] R. Gauvin, E. Lifshin, H. Demers, P. Horny, and H. Campbell, "Win X-ray: A New Monte Carlo Program that Computes X-ray Spectra Obtained with a Scanning Electron Microscope," *Microscopy and Microanalysis*, vol. 12, no. 01, pp. 49–64, Feb. 2006, doi: 10.1017/S1431927606060089.

Appendix

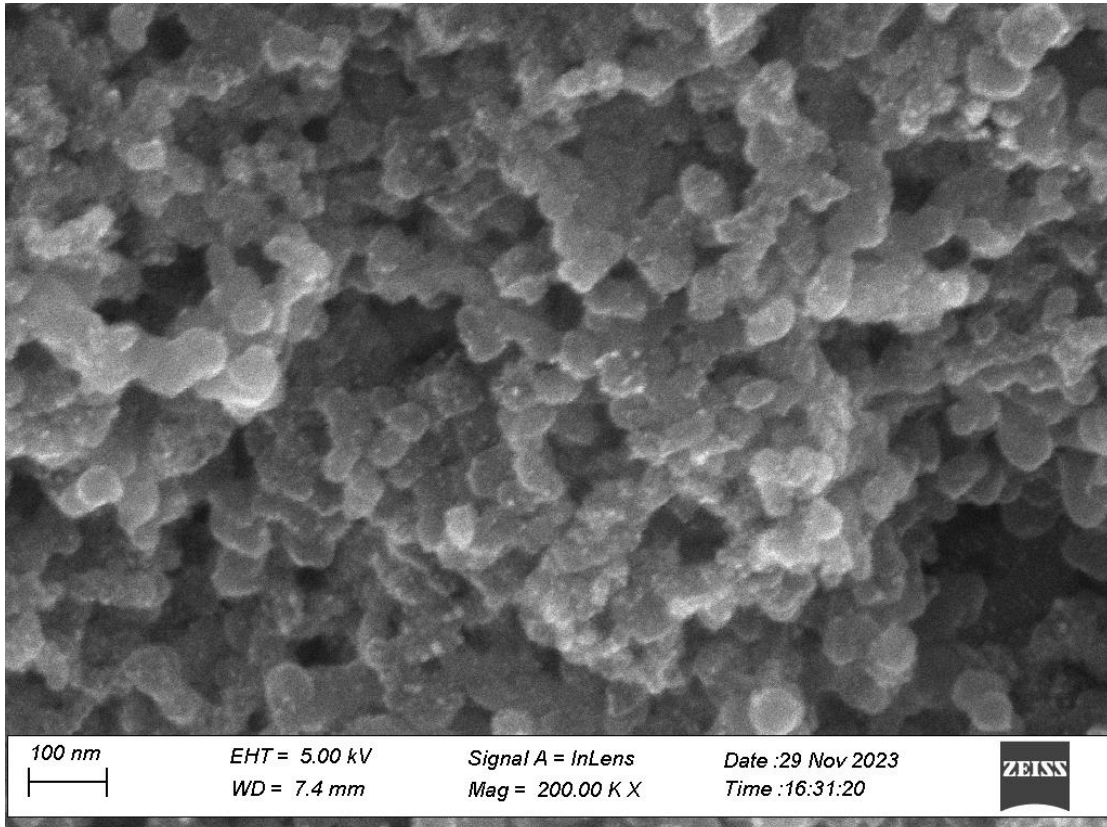


Figure 4.2d). SEM images of 50 μm coatings of Ink1 on glass fibre reinforced decal after one day of maturation, image is taken with x200 000 magnification and has a scale bar of 100 nm.

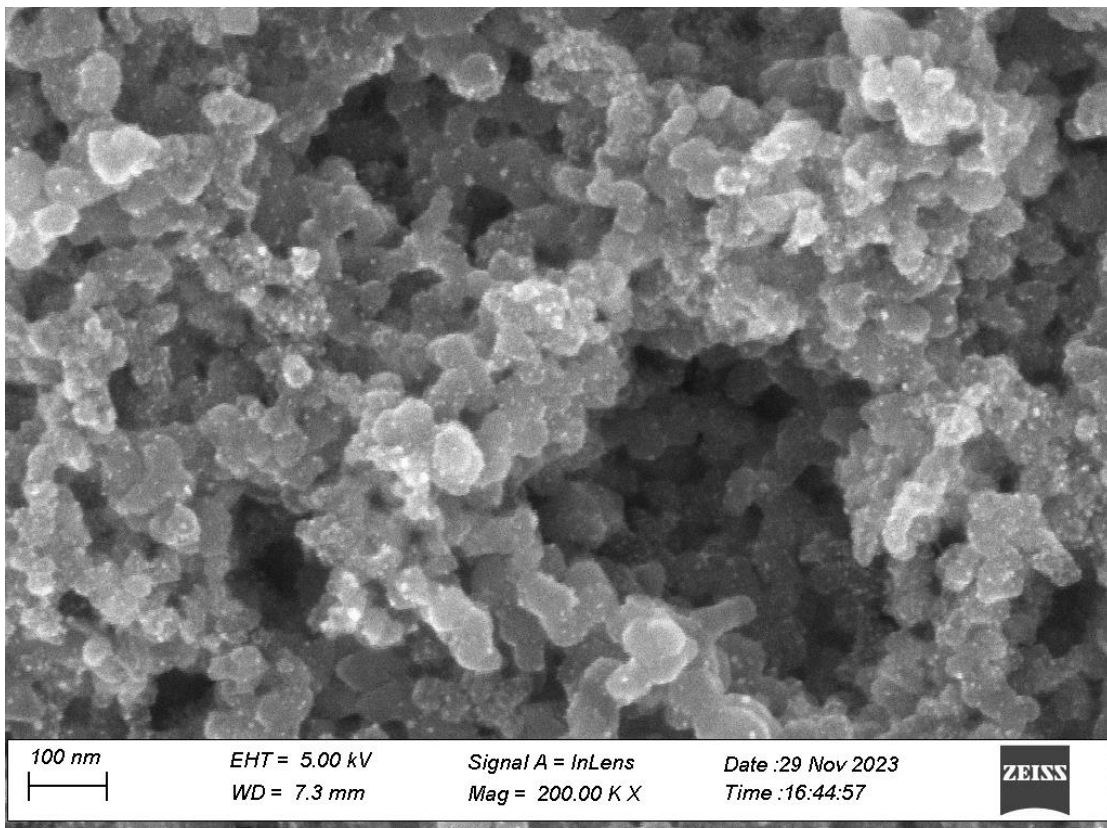


Figure 4.2e). SEM images of 50 μm coatings of Ink1 on glass fibre reinforced decal after four days of maturation, image is taken with x200 000 magnification and has a scale bar of 100 nm.

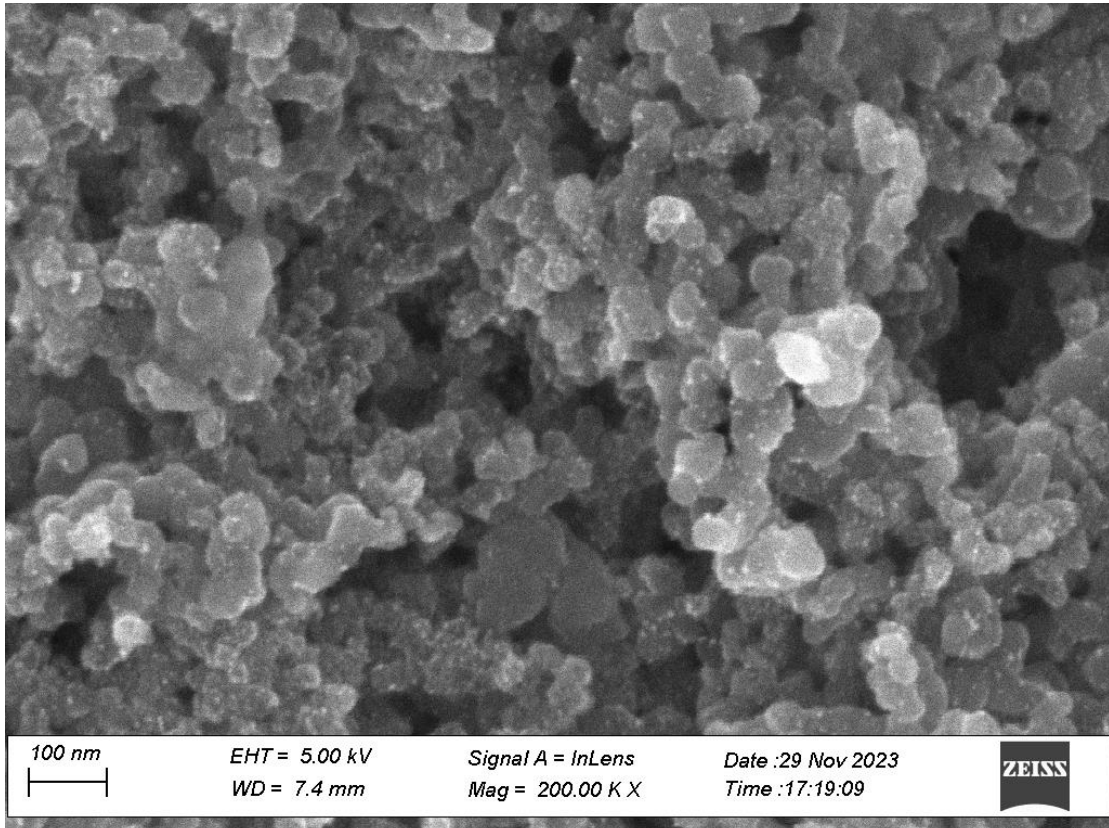


Figure 4.2f). SEM images of 50 μm coatings of Ink1 on glass fibre reinforced decal after seven days of maturation, image is taken with x200 000 magnification and has a scale bar of 100 nm.

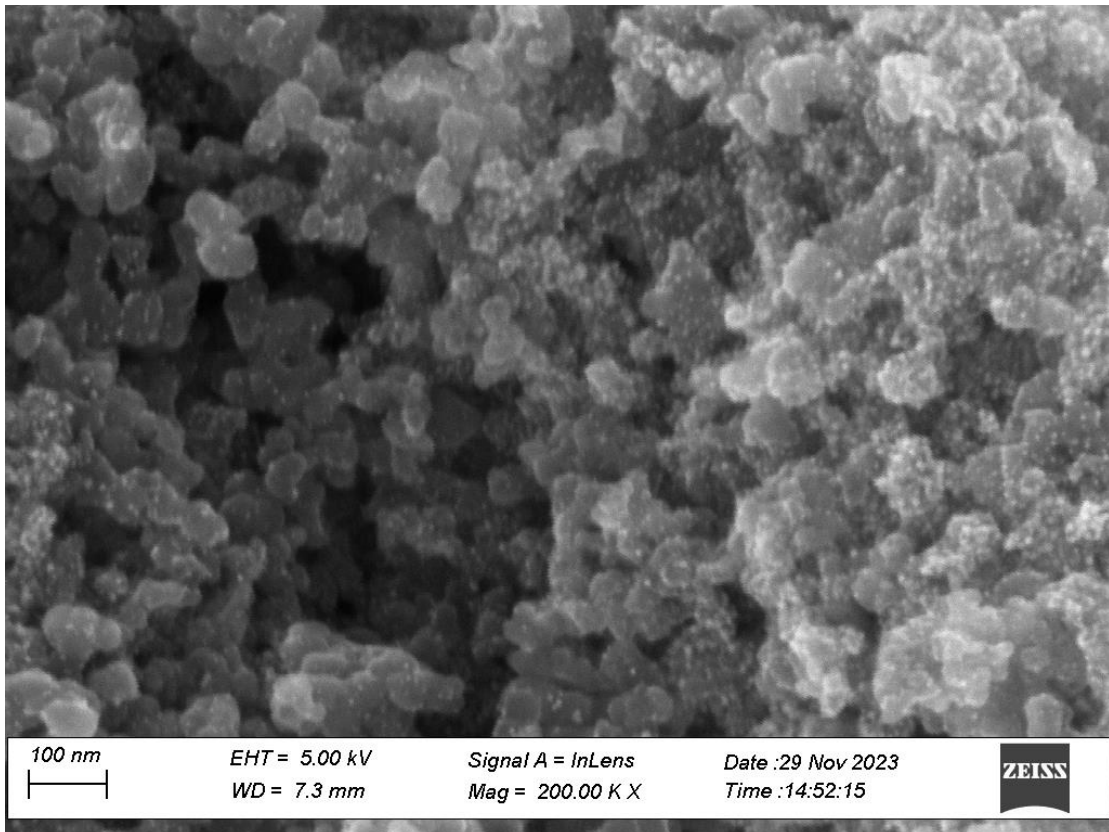


Figure 4.8c). SEM images of 150 μm coatings of Ink5 on PET reinforced decal after one day of maturation, image is taken with x200 000 magnification and has a scale bar of 100 nm.

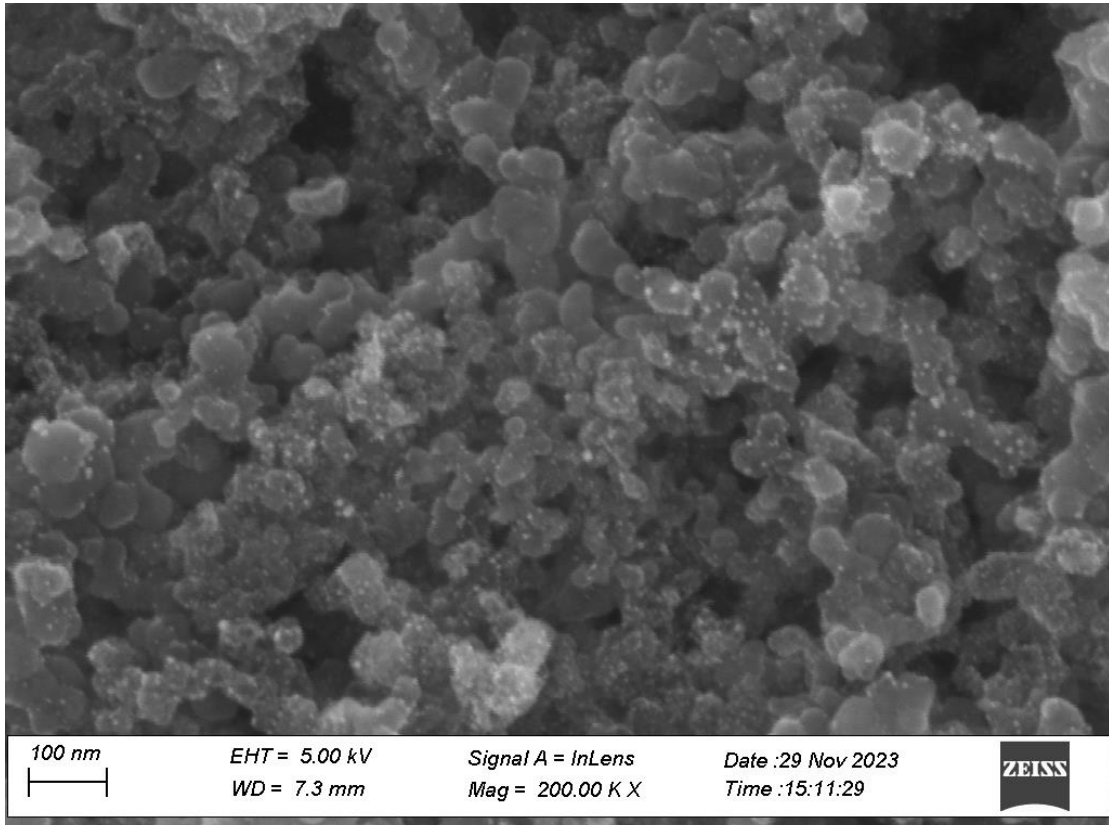


Figure 4.8d). SEM images of 150 μm coatings of Ink5 on PET reinforced decal after seven days of maturation, image is taken with x200 000 magnification and has a scale bar of 100 nm.

DEPARTMENT OF PHYSICS
CHALMERS UNIVERSITY OF TECHNOLOGY

Gothenburg, Sweden 2024
www.chalmers.se



CHALMERS
UNIVERSITY OF TECHNOLOGY